Michigan Ion Beam Laboratory

ANNUAL RESEARCH REPORT

2023

for projects conducted in 2022

Gary S. Was, Director
Kevin Field, Deputy Director
Zhijie (George) Jiao, Manager and Accelerator Scientist
Fabian Naab, Senior Accelerator Scientist
Prashanta Niraula, Accelerator Scientist
Alex Flick, Electronic Systems Engineer

2600 Draper Road
Department of Nuclear Engineering and Radiological Sciences
University of Michigan
Ann Arbor, Michigan 48109-2145
mibl.engin.umich.edu

Telephone: (734) 936-0131 Fax: (734) 764-8060

The Annual Research Report

This report summarizes the principal research activities in the Michigan Ion Beam Laboratory during the past calendar year. One hundred and thirteen researchers conducted 45 projects at MIBL that accounted for 192 irradiations and 5,713 hours of instrument time. The programs included participation from researchers at the University, other universities across the United States, corporate research laboratories, private companies, government laboratories, and various international organizations. These projects also included 5 projects funded through the Nuclear Science User Facility program. The extent of participation of the laboratory in these programs ranged from routine surface analysis to triple beam irradiations. Experiments included Rutherford backscattering spectrometry, elastic recoil spectroscopy, nuclear reaction analysis, direct ion implantation, ion beam mixing, ion beam assisted deposition, and radiation damage by proton irradiation and self-ion irradiation, dual ion irradiation and triple beam irradiation, irradiation accelerated corrosion, and irradiation creep. The following pages contain a synopsis of the research conducted in the Michigan Ion Beam Laboratory during the 2022 calendar year.

About the Laboratory

The Michigan Ion Beam Laboratory for Surface Modification and Analysis was completed in October of 1986. The laboratory was established for the purpose of advancing our understanding of ion-solid interactions by providing up-to-date equipment with unique and extensive facilities to support research at the cutting edge of science. Researchers from the University of Michigan as well as industry and other universities are encouraged to participate in this effort.

The lab houses a 3 MV Pelletron accelerator, a 1.7 MV tandem ion accelerator, and a 400 kV single ended ion accelerator that are configured to provide for a range of ion irradiation and ion beam analysis capabilities utilizing 9 beamlines, 5 target chambers and a transmission electron microscope coupled to two beamlines to provide dual beam irradiation in-situ in the TEM. The control of the parameters and the operation of these systems are mostly done by computer and are interconnected through a local area network, allowing for complete control of irradiations from the control room as well as off-site monitoring and control. This past year, a Gatan Imaging Filter (GIF) with electron energy loss spectroscopy and energy filtered TEM capabilities was added to the TF30 TEM coupled to 2 beamline to enable rapid chemical mapping/imaging methods for both ex-situ characterization efforts including full foil thickness and chemical mapping and to map chemical evolution in microstructures during in-situ TEM ion irradiation experiments.

MIBL is a Partner Facility of the National Scientific User Facility (NSUF), based at Idaho National Laboratory, providing additional opportunities for researchers across the US to access the capabilities of the laboratory. In 2016, MIBL was recognized as the top ion beam laboratory in the U.S. by the Nuclear Science User Facilities program.

Respectfully submitted,

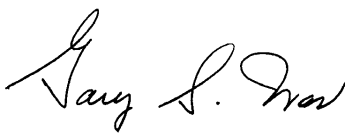

Gary S. Was, Director

Nuclear Science User Facilities (NSUF) Projects

INVESTIGATION OF THE EFFECTS OF IRRADIATION ON THE PROPERTIES OF FECRAL ALLOYS PRODUCED BY INNOVATIVE MANUFACTURING

Andrew Hoffman[1], Kai Sun[2], Zhijie Jiao[1], Gary Was[1]
[1]GE Research, Niskayuna, NY
[2]Nuclear Engineering and Radiological Sciences, University of Michigan

The objective of this proposal is to determine how the FeCrAl alloy fabrication route determines the microstructure and mechanical properties following neutron irradiation. FeCrAl alloys are fabricated through conventional melting/forging, additive manufacturing, and powder metallurgy (PM). Irradiation effects on microstructure (irradiation induced defect clusters and precipitation) and the corresponding impact on mechanical properties (hardness and embrittlement) will be evaluated. The information obtained by this study will be combined with on-going corrosion and mechanical property studies on non-irradiated samples to help guide programmatic decisions on development of fabrication methods for commercial FeCrAl alloys for accident tolerant fuel (ATF) cladding.

The wrought, additive manufactured (AM) and powder metallurgy (PM) made FeCrAl were irradiated at the Michigan Ion Beam laboratory using 2 MeV protons to 2 and 5 dpa at 380°C. Irradiation hardening as well as irradiated microstructures were characterized afterwards. Figures below show the radiation-induced segregation at the grain boundary in the PM FeCrAl sample irradiated to 5 dpa at 380°C. Enrichment of Cr/Si and depletion of Fe/Al at the grain boundary was observed.

Funding: Department of Energy (DOE) the Nuclear Science User Facilities (NSUF)

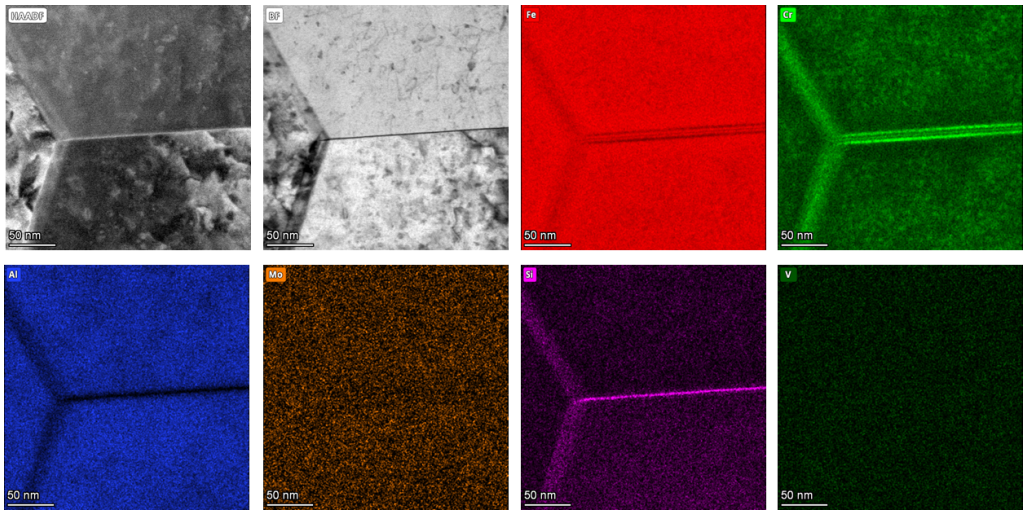

Radiation-induced segregation at the grain boundary in the PM FeCrAl sample irradiated to 5 dpa at 380°C.

IMPACT OF NICKEL DOPANT ON IRRADIATION ASSISTED CORROSION OF IRON CHROMIUM ALUMINUM ALLOY

L. Joyce[1], R. Umretiya[2], A. Hoffman[2], Y. Xie[1]
[1]School of Nuclear Engineering, Purdue University
[2]General Electric Research, Schenectady, NY 12309, USA

Iron chromium aluminum (FeCrAl) alloys are the prime accident tolerant fuel cladding candidate to replace the zirconium-based Zircaloy alloys in commercial nuclear power plants. The FeCrAl alloys are favored for the increased corrosion resistance in both operation and accident scenario conditions that they offer. As such, the corrosion characteristics of FeCrAl in both sets of conditions must be rigorously studied. Corrosion studies set on studying the formation of stable oxide layers on FeCrAl alloys in operation conditions found iron chromite ($FeCr_2O_4$) and chromia (Cr_2O_3) as the stable oxides. However, in cases where the autoclave was made of a nickel (Ni) containing stainless steel, nickel ferrite ($NiFe_2O_4$) formed on the FeCrAl alloys likely due to the nickel contamination. Nickel ferrite is a spinel oxide that may form a denser oxide layer than iron chromite or chromia, meaning more protection from metal dissolution during operation and longer operation life.

Two FeCrAl alloys were irradiated with 5.4 MeV protons while being exposed to hydrogenated water at 320 °C and 14 MPa for 24 hours to simulate pressurized water reactor (PWR) operating conditions. Both alloys were received from GE Research. One alloy contains only iron (Fe), chromium (Cr) and aluminum (Al) while the second alloy contains Ni as well. Both alloys are 17 wt.% Cr and 5.5 wt.% Al. The Ni-containing alloy has 3 wt.% Ni with the rest of the balance containing Fe. The in-situ proton irradiation-corrosion experiments were conducted at Michigan Ion Beam Laboratory (MIBL) using the Pelletron accelerator. The FeCrAl alloys were in the form of 5.4 mm diameter discs of 35 µm thickness. The protons interacted with the thin disc, but were mostly deposited in the water due to the average range of protons in FeCrAl being much larger. This helped simulate the radiolysis that would occur in a nuclear reactor and also prevented the implantation of the protons in the alloy from affecting the corrosion characteristic.

Funding information: L.J. appreciates the U.S. Nuclear Regulatory Commission (U.S. NRC) Fellowship award.

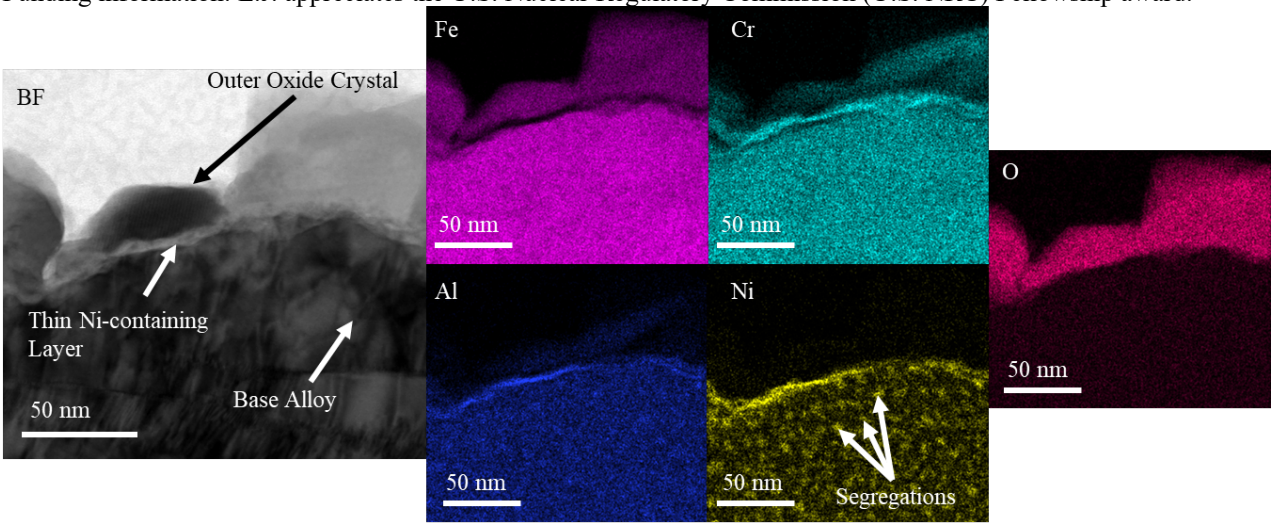

TEM bright field image with EDS maps in the irradiated region of Ni-doped FeCrAl sample. The outer oxide formed contains Fe oxide as well as some Cr oxide. Below the outer oxide is a thin layer enriched in Cr, Al, and Ni but depleted in Fe. There is little oxygen below this layer, indicating that it is a thin, continuous, protective inner oxide layer. The Ni appears to have segregated in the metal due to the irradiation.

DEFECT GENERATION AND PHASE STABILITY IN SINGLE CRYSTAL MIXED URANIUM-THORIUM OXIDES

A.R. Khanolkar[1], M. Bachhav[1]
[1]Idaho National Laboratory

Mixed actinides of uranium-thorium dioxide have been considered for advanced nuclear fuel applications; alloying traditional UO_2 fuel with thorium in hope of imparting some of the increased thermal conductivity, higher melting point, chemical stability, and proposed proliferation resistance observed in ThO_2. While fundamental data on unit phonon scattering mechanisms in either UO_2 or ThO_2 is still relatively scarce, no data presently exists for the $(U,Th)O_2$ system with high (or equal) concentrations of both actinides. Importantly, open questions remain with regards to the chemical and microstructural evolution of these mixed oxide systems under irradiation. The exsolution of UO_2 and ThO_2 domains (on the nanoscale) has been computationally proposed. This could dramatically affect the resulting thermal performance of the initially homogeneous solid solution microstructure. In this work, a series of mixed oxides of $(U,Th)O_2$ were irradiated with 2 MeV H^+ ions at 600˚C to study both defect formation and microstructure stability. Single crystals of multiple chemistries produced through hydrothermal synthesis were mounted to a custom, angled Cu plate to ensure no ion channeling effects during high temperature exposure under a raster scanned beam. Three fluences equivalent to 0.005, 0.05, and 0.5 dpa in the pre-peak plateau region targeted on identical sample matrices. Characterization of the irradiated crystals was performed using spectroscopic ellipsometry and atom probe tomography (APT). Figure 1(a) shows representative real and imaginary parts of the complex dielectric function measured using ellipsometry in an irradiated $(U_{0.5}Th_{0.5})O_2$ crystal. Absorption peaks at ~3.1 eV and ~3.3 eV were observed to shift with higher uranium content. APT analysis was also carried out on irradiated $(U,Th)O_2$ crystals to elucidate microstructural and microchemical changes due to irradiation. Representative 3D APT dataset from $(U,Th)O_2$ is show in Figure 1(b) along with a binomial distribution of O, O_2, ThO and UO_2 ions and measured composition for the irradiated crystal. Measurements of thermal property changes due to irradiation are planned.

This work was supported by the U.S. Department of Energy, Office of Nuclear Energy under DOE Idaho Operations Office Contract DE-AC07-051D14517 as part of a Nuclear Science User Facilities experiment, and the Center for Thermal Energy Transport under Irradiation (TETI), an Energy Frontier Research Center funded by the US Department of Energy, Office of Science, Office of Basic Energy Sciences.

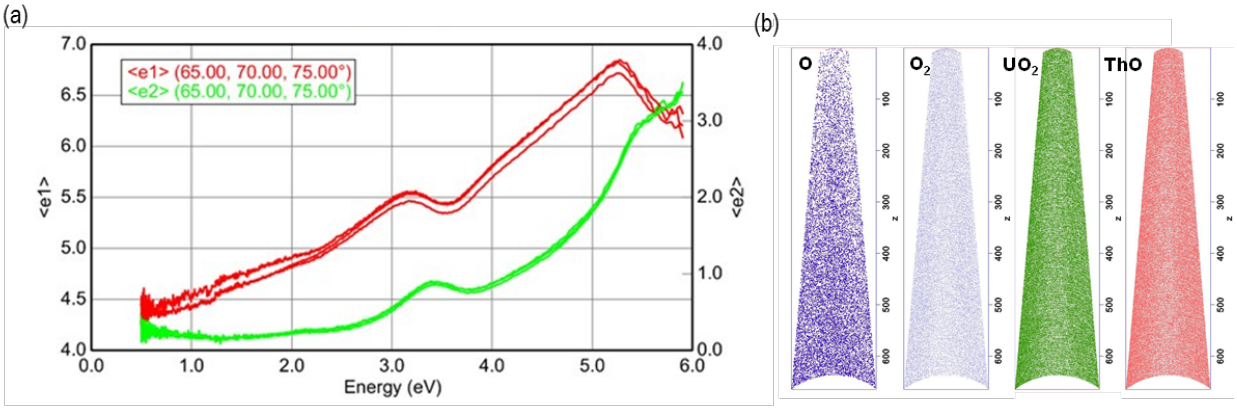

Spectral dependence of the real and imaginary parts of the complex dielectric function of a uranium-doped thorium dioxide crystal (a), and 3D distribution of O, O_2, UO_2 and ThO ions measured using atom probe tomography (b).

IRRADIATION BEHAVIOR OF NANOSTRUCTURED FERRITIC/MARTENSITIC GRADE 91 STEEL AT HIGH DOSE

H. Wen[1], J. Rittenhouse[1], Z. Jiao[2], G. Was[2], Y. Wu[3]
[1]Department of Materials Science and Engineering, Missouri University of Science and Technology
[2]Nuclear Engineering & Radiological Sciences, University of Michigan
[3]Center of Advanced Energy Studies, Idaho Falls

F/M steels such as Grade 91 are leading fuel cladding and structural materials for advanced fast reactors. Development of fast reactors require steels with enhanced irradiation tolerance and higher strength. To this end, new steels may be developed, however, such development will incur high cost and require long time. Alternatively, currently used steels may be processed by advanced manufacturing techniques to improve their performance through microstructural engineering, at relatively low cost. Such processing techniques include grain refinement through equal-channel angular pressing (ECAP) to achieve an ultrafine-grained microstructure (UFG, 100 nm < grain diameter < 1 μm) and high-pressure torsion (HPT) to achieve a nanocrystalline microstructure (NC, grain diameter < 100 nm). Grain boundaries have been found to act as sinks to irradiation-induced defects. It follows that increasing the fraction of grain boundaries improves the efficiency in which such irradiation-induced defects are absorbed, leaving the microstructure relatively intact compared to a traditional coarse-grained counterpart.

To study the irradiation behavior of Grade 91 steel with a range of grain sizes at high dose and further assess the use of such material for applications in LWRs and advanced reactors, three sets of samples were irradiated using the 3 MV National Electronics Corporation Pelletron accelerator at the Michigan Ion Beam Laboratory at four different temperatures, RT, 300, 400, 450, and 500ºC to a dose of 200 DPA using Fe^{2+} ions. The three sample sets consist of the following: (1) conventional CG Grade 91 steel; (2) ECAP processed UFG Grade 91 steel; (3) HPT processed NC Grade 91 steel. The Michigan Ion Beam Laboratory was selected for its extremely capable staff and the ability to perform self-ion irradiation of the G91 steel to a high dose at multiple, monitored temperatures. Those irradiations have been completed and the RT and 450ºC samples have been sent to the Center of Advanced Energy Studies (CAES) for post irradiation examination (PIE). Only the RT and 450ºC samples were selected for PIE due to time and budget constraints. PIE is in progress and will include nanohardness measurements and characterization using advanced transmission electron microscopy (TEM) techniques including scanning TEM, energy dispersive X-ray spectroscopy, high-resolution TEM, and precession electron diffraction. Such characterization will compare the effects of radiation within the grain refined microstructures to that of the irradiated CG microstructures. Such aspects of comparison include radiation-induced hardening, solute segregation, and precipitation. Following PIE, detailed analysis of data will proceed, and the results will be compiled into one or more publications.

HYDROGEN-RETENTION OF YTTRIUM-HYDRIDE UNDER HIGH-TEMPERATURE PROTON IRRADIATION

T. Lach[1], S. Taller[2], F. Naab[3], T. Koyanagi[1]
[1]Materials Science and Technology Division, Oak Ridge National Laboratory
[2]Nuclear Energy and Fuel Cycle Division, Oak Ridge National Laboratory
[3]Michigan Ion Beam Laboratory, University of Michigan

The compactness of nuclear microreactors can only be obtained using dense material components for the nuclear fuel, core heat removal components, reflectors, and moderators. Solid moderators contribute largely to the compactness using hydrogen-bearing materials, such as metal hydrides, offering the highest moderation per unit volume. Yttrium hydride is an attractive option for a metal hydride neutron moderator due to a very high atomic density of hydrogen and high temperature stability without radiation. Hydrogen retention governs the moderation of neutrons but also prevents the buildup of released hydrogen gas. However, its phase stability and hydrogen retention capability under high temperature irradiation is largely unknown.

Bulk yttrium hydride with nominal composition of $YH_{1.8}$ was irradiated with either 1 MeV or 2 MeV protons to 0.2 dpa at nominal temperatures of 300 °C or 580 °C. Before and after each ion irradiation, elastic recoil detection analysis (ERDA) was performed at MIBL using 2.85 MeV He^{2+} ions at room temperature in the IBM geometry to measure the hydrogen concentration at multiple spots on the surface. Preliminary comparisons of ERDA spectra before and after irradiation are shown in the figure. After irradiation at 300 °C, the hydrogen concentration appears to be consistent with the pre-irradiation concentration regardless of proton energy. At 580 °C, 1 MeV protons appeared to result in more hydrogen loss in the near surface layers than 2 MeV protons. Quantification of the hydrogen concentration is on-going.

This work was supported by the U.S. Department of Energy, Office of Nuclear Energy under DOE Idaho Operations Office Contract DE-AC07-051D14517 as part of a Nuclear Science User Facilities experiment.

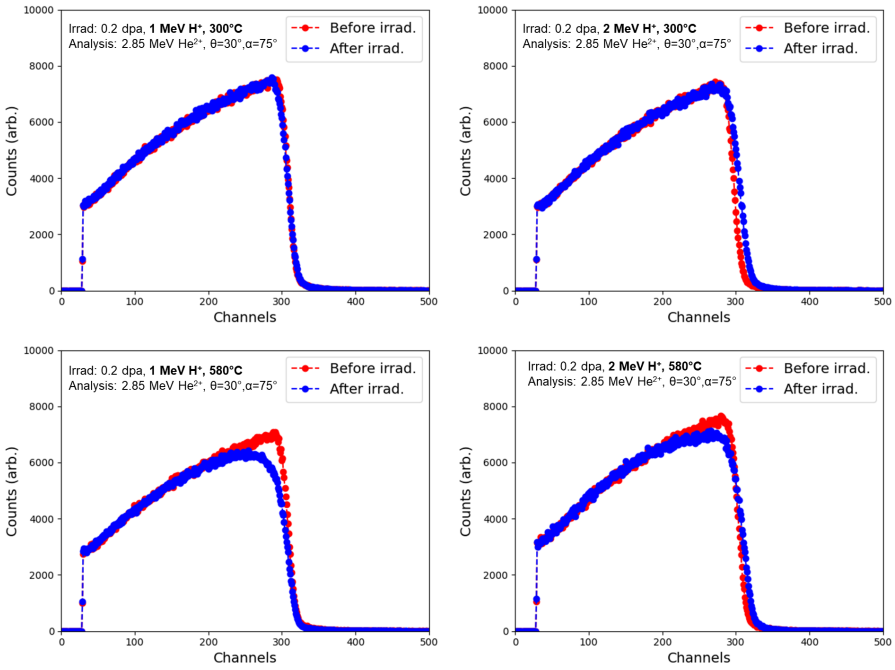

Collected elastic recoil detection analysis (ERDA) spectra for $YH_{1.8}$ showing qualitative comparisons for each irradiation condition before and after irradiation to 0.2 dpa. Note the spectra have been scaled to minimize the difference in channels 25-100 representing the "bulk" hydrogen concentration.

RESEARCH PROJECTS

USING IN SITU ENERGY-FILTERED TEM ION IRRADIATIONS TO EVALUATE PHASE STABILITY IN ADVANCED ALLOYS

Robert Renfrow[1], Kai Sun[1], Fabian Nabb[1], Caleb Massey[2], Ying Yang[2], Kevin G. Field[1]
[1]Department of Nuclear Engineering and Radiological Sciences, University of Michigan
[2]Oak Ridge National Laboratory, Oak Ridge, Tennessee

A common method for increasing the radiation tolerance of reactor structural materials is to tailor the microstructure to contain finely dispersed second-phase particles that act as trapping sites for radiation-induced defects. Two candidate high-chromium (8-12%) ferritic alloys being considered for advanced nuclear applications were irradiated using Kr and He ions to mimic radiation damage and gas production that occurs in materials during reactor operation. The first material was the Oak Ridge Fast Reactor Advanced Cladding (OFRAC) alloy, which is an oxide-dispersion strengthened alloy with (Y,Ti)O nanoclusters. The second material was another material developed at Oak Ridge, the Additively manufactured Nanostructured Alloy 2 (ANA2), a Fe-8.2Cr-2.1Mn alloy designed using computational thermodynamics to produce finely dispersed ($x10^{22}$ m^{-3}) VN type precipitates.

Below are Fe-M jump ratio micrographs from single and dual ion irradiations of OFRAC to 5 dpa at consistent dose rates with and without He co-injection. There is perceived instability of smaller Ti-O nanoclusters, suggesting that size affects radiation tolerance of particles in the alloy matrix.

This work was supported by internal funds to University of Michigan and by the Department of Energy Nuclear Energy under Award Number DE-NE0009122, a General Scientific Infrastructure grant

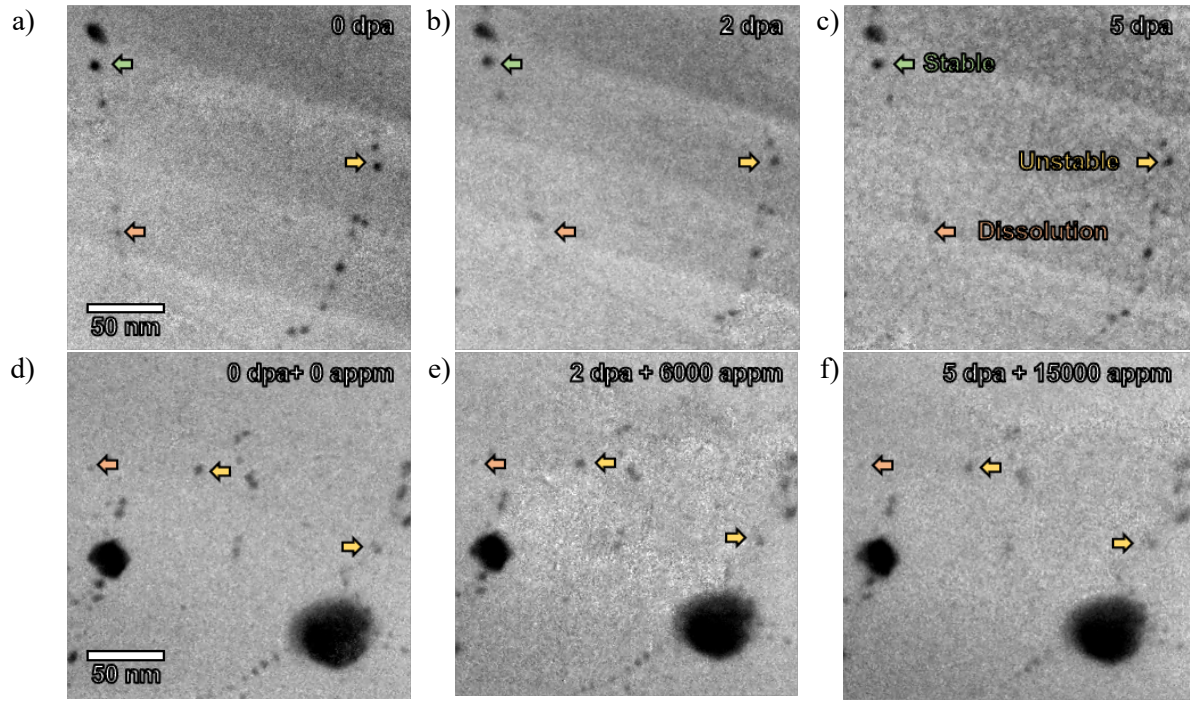

EFTEM Fe jump ratio maps for two separate in-situ TEM ion irradiation experiments: (a-c) single ion beam irradiation at a dose rate of 3×10^{-4} dpa/s, (d-f) dual beam irradiation at a dose rate of 3×10^{-4} dpa/s at doses of (a,d) prior to irradiation, (b,e) 2 dpa, and (c,f) 5 dpa. All irradiations performed at room temperature. Figures contributed by K.G. Field.

MICROSTRUCTURAL EVOLUTION AND HARDNESS CHANGES IN ION IRRADIATED NI-BASED SUPERALLOYS

Qinyun Chen[1*], Ryan Thier[1], Yan-Ru Lin[2], Ling Wang[3], Steven J. Zinkle[1,2]
[1] University of Tennessee, Knoxville, TN 37996, United States of America
[2]Oak Ridge National Laboratory, Oak Ridge, TN 37831, United States of America
[3] SLAC National Accelerator Laboratory, Menlo Park, CA 94025, United States of America

Nickel-based superalloys are promising structural material candidates for molten salt reactors. However, historic Ni superalloys have generally exhibited severe radiation-induced degradation (mainly due to instabilities in Si-containing gamma prime precipitates). We have examined radiation effects in several high-performance commercial Ni superalloys: Haynes 282 and Haynes 244 with different heat treatments encompassing solid solution and precipitation-strengthened approaches. The precipitates in the selected alloys are expected to exhibit suitable radiation resistance. These materials were irradiated with 8 MeV Ni ions up to midrange doses of 1 and 10 dpa at 600℃ and 750℃.

The microstructural changes were characterized with cross-section TEM, and mechanical property changes were analyzed using nano-indentation. Microstructural information was summarized regarding the size and density of precipitates and dislocations as a function of irradiation temperature, doses, and precipitate types. The gamma-prime precipitates in Haynes 282 seem to have strong radiation resistance since there is no apparent difference in the size distribution in irradiated and pristine regions. In comparison, Haynes 244 is more sensitive to radiation effects, where radiation-enhanced precipitation and ballistic dissolution dominate at different doses. More details will be available in a journal article.

This work was supported by the U.S. Department of Energy, Nuclear Energy University Program Contract DE-NE0008971.

METHODS FOR EXTRACTION AND SEPARATION OF HELIUM-3 FROM THE MOON

J. Chad, R. Halphen, H. Hare, J. Huerta, G. Tubay, K. Zheng, and K. Weintraub
Multidisciplinary Design Program (MDP) project team, University of Michigan

He-3 is a rare isotope on Earth but abundant on the Moon due to the solar wind constantly bombarding the moon with volatile gases, making lunar extraction increasingly more popular due to the decreasing supply of He-3 on Earth. There have been advancements in the development of a lunar mining system to extract and collect the desired resources, but there has not been much work done in understanding the mechanisms behind the extraction of the volatile gases from the lunar regolith and the separation of the He-3 from the rest of the volatile gases.

One way of extracting the volatile gases is by heating the lunar regolith to thermally excite the implanted gases, allowing them to be extracted from the regolith. Another way that has not been thoroughly studied is extraction using mechanical forces. In order to study this mechanism, our group used the 400 kV ion implanter at MIBL to implant a concentration of He-4 (an appropriate surrogate due to similar diffusive properties) similar to the concentration of He-3 in the lunar soil into our lunar regolith simulant to study the extraction of He-3. Heating the regolith for 10 minutes at 100 °C intervals between 0-1200 °C showed peaks in the He-4 release occurring at 400 and 800 °C, indicating two types of He-4 release. The He-4 released at 400 °C could possibly be extracted using mechanical forces, since the He-4 released at this temperature are most likely implanted in the grain boundaries of the regolith.

Our group also worked on the separation of the volatile gases from the lunar regolith after extraction. Since there are many other gases contained in the solar wind besides He-3 and He-4 with much larger sizes, our group is proposing the use of graphene sheets to extract He-3 and He-4 from the rest of the other volatiles. Graphene is theorized to be very effective because the permeability of a membrane is inversely proportional to its thickness, so a one-atom thick sheet of graphene may be considered as the most effective gas separating device possible.

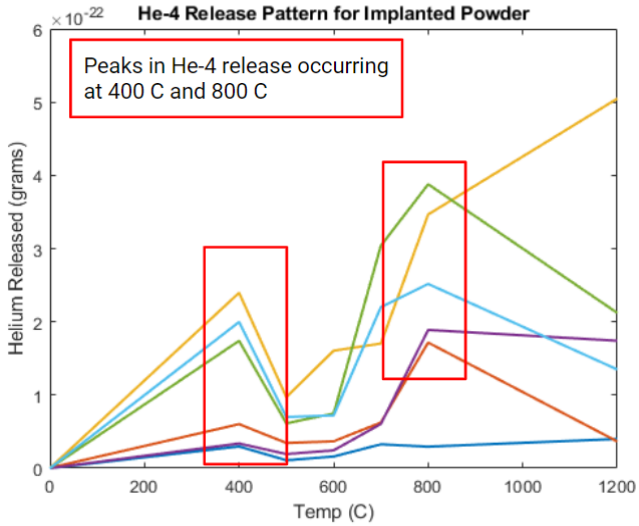

Helium release as a function of temperature.

HIGH-TEMPERATURE OXIDATION MECHANISMS OF TITANIUM ALLOYS

T. Valenza[1] and E. Marquis
[1]Department of Materials Science and Engineering, University of Michigan

Developing structural alloys with high strength, low weight, and good high-temperature stability is key to enabling advances in transportation and aerospace in particular, while addressing environmental concerns such as fuel consumption and CO_2 emissions. Titanium alloys are particularly promising candidate materials because of their high strength-to-weight ratio and good corrosion resistance. However, accelerated oxidation at high temperatures remains a key limitation. Oxidation is typically considered detrimental because it degrades mechanical properties and therefore jeopardizes performance of structural titanium alloys. Titanium metal becomes brittle due to oxygen enrichment and transforms into oxide with poor load-bearing capability. As early as 1955, Maynor et al. demonstrated that the oxidation rate of titanium could be slowed by alloying with small amounts of other elements [1]. However, in the decades since, very limited progress has been made toward understanding the mechanisms behind the beneficial roles of dilute alloying elements. Specifically, one mechanism repeated throughout the literature is that Si [2] or Nb [3] alloying additions dope the rutile TiO_2 oxide scale, changing the stoichiometry in a way that slows transport through the oxide scale and thereby slowing oxide scale growth. However, differences in stoichiometry have not been confirmed experimentally.

Therefore, we oxidized titanium with dilute Si or Nb additions and performed RBS and/or NRA on the TiO_2 oxide to measure stoichiometry. However, it was not possible to determine stoichiometry, as small differences in fitting the data produced differences on the order of possible stoichiometry differences. Since the results were inconclusive, they have not been included in any presentations and will most likely not be published.

[1] H.W. Maynor, B.R. Barrett, and R.E. Swift, “Scaling of titanium and titanium alloys,” Wright Air Development Center, WADC Tech. Rep. 54-109, 1955.
[2] A.M. Chaze and C. Coddet, “Influence of silicon on the oxidation of titanium between 550 and 700°C,” *Oxidation of Metals*, vol. 27, no. 1, pp. 1–20, 1987.
[3] P. Pérez, V.A.C. Haanappel, and M.F. Stroosnijder, “The Effect of Niobium on the Oxidation Behavior of Titanium in Ar/20% O_2 Atmospheres,” *Oxidation of Metals*, vol. 53, no. 5, pp. 481–506, 2000.

ION IRRADIATIONS FOR ACCELERATED CREEP TESTING USING TAPERED 316 SPECIMEN GEOMETRIES

M. M. Warwick[1], C.A. Hirst[1], W. Peterson[1]
[1]Department of Nuclear Engineering and Radiological Sciences, University of Michigan

Currently, materials qualifications for use in nuclear applications takes decades and with the influx of proposed advanced reactor design concepts, we need materials that can withstand the extreme conditions. Creep, a plastic deformation under high temperatures ($0.3\ T_m < T < 0.5\ T_m$) and applied stresses below the yield stress, takes decades to appear and is the leading cause of structural material failure in nuclear reactors. Current single stress-state ion irradiations take approximately 150 hours, which exponentially increases the number of required irradiation-temperature-stress experiments needed to explore the fundamental mechanisms of irradiation creep. This work explores the feasibility of the tapered specimen geometry to achieve two distinct stress states within the gauge length, and ultimately, two distinct creep regimes; significantly reducing the number of experiments without compromising the condition space.

The specimen is a thin foil of annealed 316 SS with a thickness of 25 um. The specimen geometry is a tapered dog-bone and an irradiated gauge length of 5 mm. The irradiation area included a 4 mm and 2 mm gauge width, with applied stresses of 158 MPa and 316 MPa, respectively; these stresses were achieved by attaching tungsten dead-weights to the specimen holder. Thermal and irradiation creep experiments were completed at 500°C for approximately 150 hours, with the irradiation creep test using 3 MeV H^+ ions to a damage level of 0.4 dpa using a 3 MV National Electronics Corporation Pelletron accelerator in Michigan Ion Beam Laboratory (MIBL). The primary strain monitoring method was through a laser speckle extensometer (LSE), an optical strain measuring system developed by Messphysik, which utilized a 532 nm wavelength green laser that shined upon the specimen surface and reflected into the camera creating a series of speckle patterns that were then recorded by the accompanying software.

With the given applied stresses and temperature, preliminary results show that the 4 mm gauge width is within the irradiation creep regime and the 2 mm gauge width is within the dislocation creep regime. Further irradiation experiments and microscopy investigations are planned.

This material is based upon work supported by the Department of Energy Nuclear Energy under Award Number DE-NE0009289 and under contract with Idaho National Laboratory under Award Number 253513.

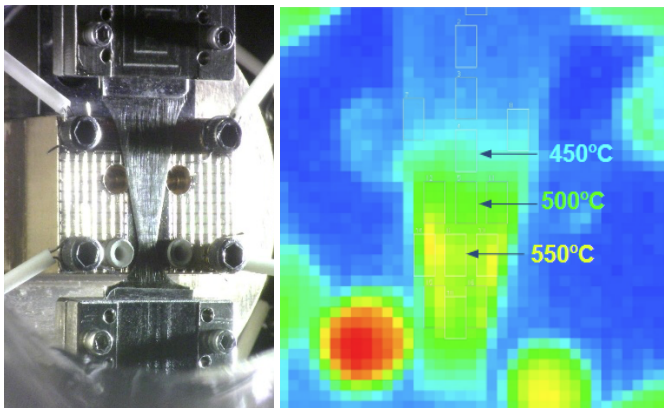

Left: Pre-irradiation set-up of the tapered sample. The tungsten dead-weights are attached to the sample using a clevis rig and friction clamps. The sample surface was roughened to increase the contrast of the laser that reflects off the sample. Right: A thermal image from the FLIR during the irradiation, where most of the irradiation area is approximately 500°C. The sample was pre-heated to 500°C to adequately calibrate the FLIR camera.

RADIATION INDUCED SEGREGATION IN TI-B SYSTEMS

Shuguang Wei[1], Hongliang Zhang[2], Izabela Szlufarska[1]
[1]Department of Materials Science and Engineering, University of Wisconsin–Madison
[2]Department of Engineering Physics, University of Wisconsin–Madison

Binary titanium borides exhibit many excellent properties, such as high melting temperatures, high neutron capture cross-section, and chemical inertness and they are considered to be promising for nuclear application, including neutron shielding and plasma facing components. Based on Ti-B binary phase diagram, Ti-B forms three stable line compounds (TiB, Ti_3B_4 and TiB_2). As was previously shown for SiC, unbalanced defect fluxes to the grain boundary (GB) can induce local changes in composition, even though SiC forms a line compound and has a strong thermodynamic driving force to be stoichiometric. The goal of this project was to investigate the existence and the extent of this type of radiation-induced segregation (RIS) in Ti-B systems. TiB and TiB_2 are selected for the studies of radiation induced damage and possible RIS. TiB was synthesized using hot pressing and TiB_2 was prepared using both hot pressing as well as arc melting. For TiB and TiB_2 sample synthesized using hot pressing, samples were irradiated with a 6.00MeV silicon ion beam incident at 0° to the normal using the tandem accelerator at Ion Beam Lab, University of Michigan. The irradiation was performed at 150°C and at 300°C. The typical irradiation flux was kept at ~1.2×10^{12} ions·cm^{-2}·s^{-1}. The irradiation fluence delivered to the samples was 1.3×10^{16} ions·cm^{-2} at 150°C (low dose) and 2.6×10^{16} ions·cm^{-2} at 300°C (high dose). For arc-melted TiB_2 samples, they were irradiated with a 3.00MeV silicon ion beam at 300°C and 600°C using the tandem accelerator in MIBL. The irradiation induced damage in hot pressed TiB and TiB_2 were studied based on TEM data and they are shown in the figure below. As shown in the figure, TiB sample irradiated at 150°C exhibited clear amorphous band, while TiB_2 samples irradiated at the same condition remained crystalline even at the damage peak, suggesting that TiB_2 has better radiation resistance as compared to TiB when irradiated at low temperatures. When temperature increased to 300°C, both TiB and TiB_2 remained crystalline even when the damage dose was doubled. In addition, we found that there is a significant RIS in TiB_2 and using atomistic simulations we have shown that RIS is due to formation of B_{Ti} antisites and fast diffusion of B vacancies to GBs. The results are being prepared for publication.

The authors gratefully acknowledge support from the Department of Energy Basic Energy Science Program (grant # DEFG02–08ER46493).

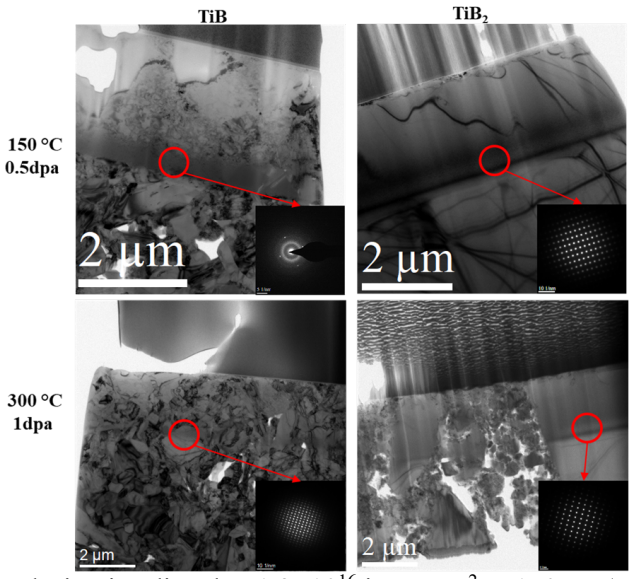

BFTEM images of TiB and TiB_2 irradiated at 1.3×10^{16} ions·cm-^{2} at 150 °C (top row), and at 2.6×10^{16} ions·cm^{-2} at 300 °C (bottom row).

IRRADIATION INDUCED DAMAGE IN TIC_X WITH DIFFERENT CARBON CONTENT

Shuguang Wei[1], Hongliang Zhang[2], Izabela Szlufarska[1]
[1]Department of Materials Science and Engineering, University of Wisconsin–Madison
[2]Department of Engineering Physics, University of Wisconsin–Madison

Titanium carbide is a high temperature ceramic considered to be promising for applications as a structural component in nuclear reactors due to such outstanding properties of this material as high melting point, excellent mechanical properties, and good corrosion resistance. Understanding of defects recovery processes in TiC is still limited due to its complex energy landscape. In addition, the fact the TiC can be stable within a wide range of carbon stoichiometries makes the defect recovery processed even more complex. The goal of this project is to understand the impact of carbon stoichiometry on radiation-induced defects.

Toward this goal, thin film TiC_x samples with different carbon to titanium ratio (x) were synthesized using radio frequency magnetron sputtering by depositing Ti-C target to Al_2O_3 substrate. Composition was measured using XPS by comparing the ratio of the area under C 1s peak to the area under Ti 2p peaks for each sample. All TiC_x samples were then irradiated with a 3.00MeV silicon ion beam incident at 0° to the normal using the tandem accelerator at Ion Beam Lab, University of Michigan. The irradiation was performed at 300°C and 600°C. The typical irradiation flux was kept at ~8.17×10^{11} ions·cm^{-2}·s^{-1}. The irradiation fluence delivered to the samples was 1.47×10^{16} ions·cm^{-2} at 600°C. The damage induced by irradiation was studied by analyzing the black spot defects in TiC_x samples using TEM. TEM images of $TiC_{0.67}$, $TiC_{0.73}$ and $TiC_{0.80}$ before irradiation and after irradiation at 300 °C to a damage level of 1dpa are shown in the figure below. We are in the process of interpreting the data.

The authors gratefully acknowledge support from the Department of Energy Basic Energy Science Program (grant # DEFG02–08ER46493).

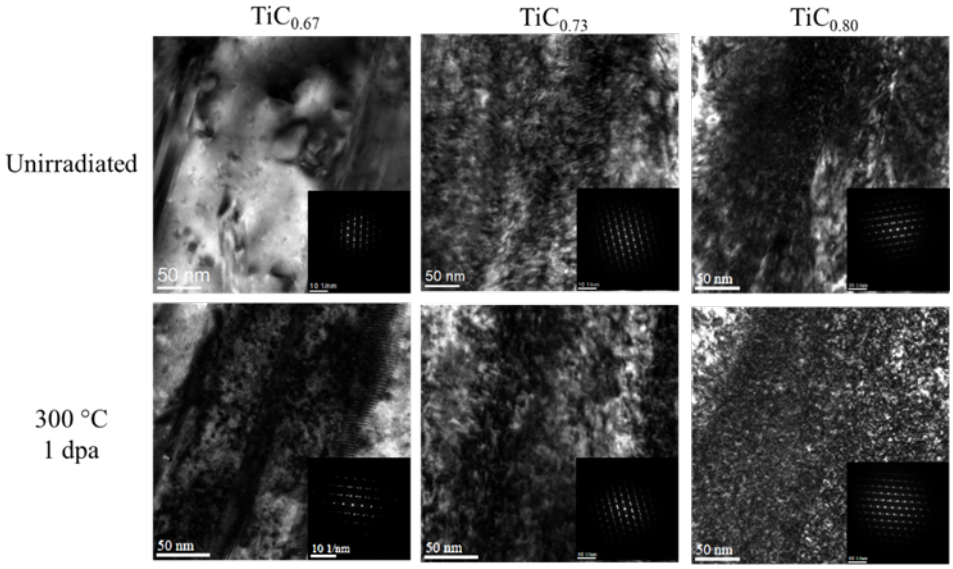

Bright field TEM images of TiC_x samples before irradiation (top row), and at 1.47×10^{16} ions·cm^{-2} at 300 °C (bottom row). The selected area electron diffraction analysis were performed on the region that contains the grains in the images, which reaches a damage dose of ~1 dpa when irradiated at 300 °C.

BALLISTIC DISSOLUTION OF NANO-SCALE PRECIPITATES IN FE-BASED BINARY ALLOYS

Y. Zhao[1], S.J. Zinkle[1,2]
[1]University of Tennessee, Knoxville, TN,
[2]Oak Ridge National Laboratory

Displacement cascades that form during heavy ion irradiations are known to cause ballistic dissolution and affect the stability of precipitates. To quantify the rate of ballistic dissolution, both FeCu (containing ~0.7%Cu) and Fe-18Cr specimens were aged to form nm-scale solute precipitates. These aged specimens were then irradiated by 8 MeV Fe ions at -123 °C – room temperature (R.T.) to final doses of 0.1 - 0.6 dpa. These low temperatures were chosen to minimize the effect of back diffusion of ejected solute. Solute atom distributions after irradiations were studied by APT.

Three irradiation conditions were selected: one at -123 °C, mid-range dose (at 1μm depth) of 0.1 dpa, two at R.T. and final doses of 0.2 and 0.6 dpa, respectively. The dose rate was 3×10^{-4} dpa/s. All experiments have been completed using defocused beams of 8 MeV Fe ions. Figure (a) shows the damage profile and injected ions concentrations. Temperature alignment was done through thermocouples, spot-welded on the FeCr guidebars, and it was monitored by infrared camera through the whole irradiation. Pressure and beam currents were recorded during the irradiation experiments. Multiple specimens containing pre-existing precipitates formed from thermal aging were irradiated on each stage. Their precipitate distributions characterized by APT are presented in Figure (b). Comprehensive characterization and analysis of the sample microstructures evolution after irradiations is in progress.

This work was supported by the Office of Fusion Energy Sciences, U.S. Department of Energy.

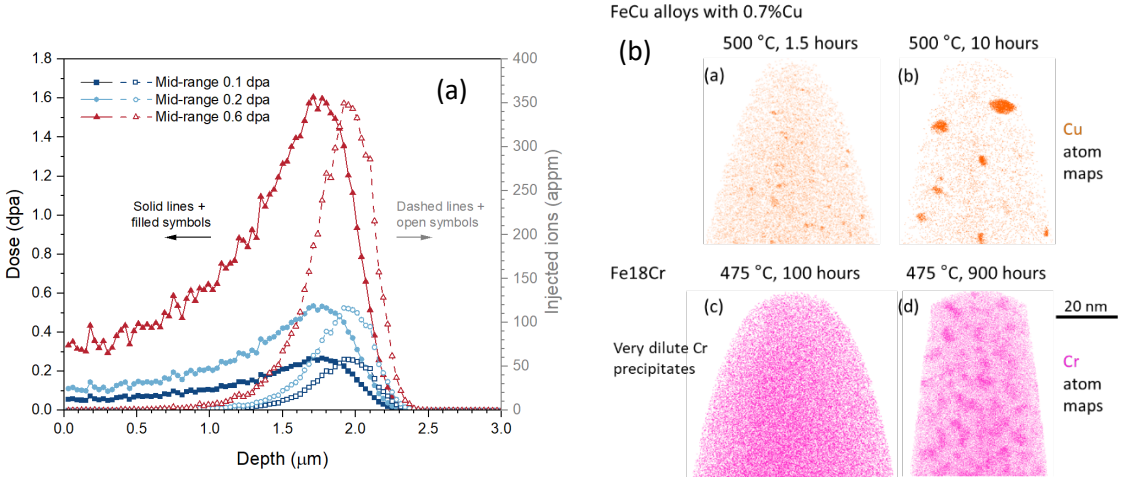

SRIM based estimates of depth profile of displacement damage in dpa and implanted Fe ions concentration in pure Fe (a), and precipitate distributions in specimens before irradiation (b).

IN SITU ION IRRADIATION STUDY OF BA- AND CS-HOLLANDITE WASTE FORMS

Yuhan Li[1], Kai Sun[1] and Lumin Wang[1,2]
[1]Department of Materials Science and Engineering, University of Michigan
[2]Department of Nuclear Engineering and Radiological Sciences, University of Michigan

The ceramic materials with the structure of hollandite mineral have been proposed to serve as the nuclear waste form to host radionuclides (e.g., Cs) in the high-level nuclear waste (HLW) due to high waste loading capacity and excellent chemical durability. The waste form has demonstrated high structural stability under ionizing radiation from 200 and 300 kV electron beam irradiation. The purpose of this work is to study the effects of displacement damage that may be induced by alpha-decay recoils of the transuranic elements (TRU) in the Ba- and Cs-end members of the Ba/Cs-Fe/Ti hollandite waste form with *in situ* TEM analysis. 1.2 MeV Kr^{3+} ion irradiation was conducted at 200°C for the study. The two samples tested have the chemical compositions of $Ba_{1.33}Fe_{1.33}Ti_{6.67}O_{16}$ (H1) and $Cs_{1.33}Fe_{1.33}Ti_{6.67}O_{16}$ (H4), respectively.

Figure 1 compares the selected area electron diffraction patterns (SADP) of the two specimens obtained by *in situ* TEM during the ion beam irradiation. The diffraction spots from the crystalline structure gradually diminished while the amorphous halo ring appeared and became dominant with the increasing irradiation dose, indicating the progressive process of the solid-state amorphization. The critical amorphization dose, when the Bragg spots completely disappeared in the diffraction pattern, are 0.176 and 0.289 dpa, for the Ba- and Cs-end members (H1 and H4) respectively. The curves of accumulation of amorphous fraction with increasing irradiation dose for the two hollandite compositions are plotted in Figure 2. The Cs-end member of hollandite took 60% higher dose than the Ba-end member to become fully amorphous. The mechanism for the composition control of radiation tolerance of the hollandite waste form is under further investigation.

This work was supported as part of the Center for Hierarchical Waste Form Materials (CHWM), an Energy Frontier Research Center funded by the U.S. Department of Energy, Office of Science, Basic Energy Sciences under Award No. DE-SC0016574.

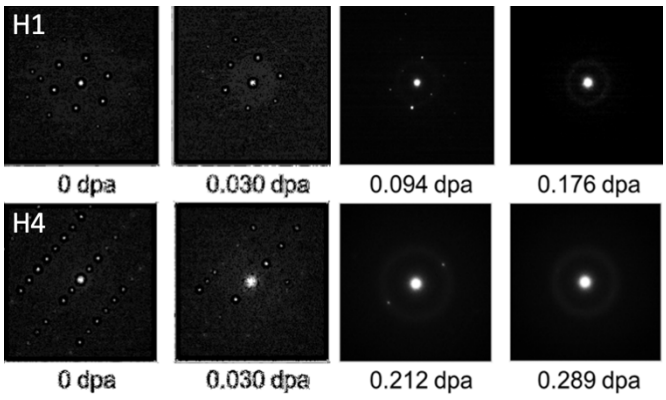

Fig. 1 Progressive amorphization process of Ba (H1) and Cs (H4) end members of hollandite composition irradiated with 1.2 MeV Kr^{3+} ions at 200ºC.

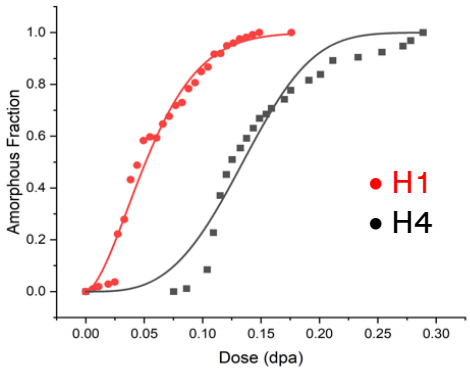

Fig. 2 Amorphous fraction vs. dose curves for the two hollandite samples under the Kr^{3+} ion irradiation.

INVESTIGATION OF ION IRRADIATION EFFECTS ON MINERAL ANALOGUES OF CONCRETE AGGREGATES

Zehui Qi[1], Steven John Zinkle[1,2], Yann Le Pape[2], Elena Tajuelo Rodriguez[2], Xin Chen[3], Arnaud Bouissonnie[3], Gaurav Sant[3]
[1]The University of Tennessee, Knoxville
[2]Oak Ridge National Laboratory
[3]University of California, Los Angeles

Amorphization and radiation induced volume expansion (RIVE) are considered as the primary causes that limit long-term performance of nuclear concrete. These irradiation changes can vary for different aggregates used in concrete. To develop a consistent knowledge of irradiation effects in concrete, selected mineral analogues of concrete aggregates (limestone, marble and quartzite) were irradiated by Ni ions to the dose that should induce full amorphization at room temperature. Irradiation induced cracks were characterized by SEM and EBSD. GIXRD and nanoindentation were used to observe amorphization, RIVE and hardness change.

13 MeV Ni irradiation was performed using a 3.0 MV tandem accelerator at Michigan Ion Beam Lab (MIBL) to a fluence of 5×10^{15} ion/cm^2 at room temperature (< 50 ℃) that could produce surface dose of ~0.2 dpa in SiO_2. Only one quadrant of each sample (~2.5 mm x 2.5 mm) was irradiated which provided direct comparison between irradiated and pristine surfaces. For quartz phase, there is irradiation induced cracking and pores formation that mainly along grain boundaries in quartzite, which might be due to anisotropic RIVE of quartz grains. Also, there is slight lattice shrinkage (~0.24%) occurred in the calcite matrix of Ni irradiated limestone, which might be due to the RIVE of the surrounding quartz inclusions. Moreover, the GIXRD peak is not obvious with ~80% peak broadening, and ~33% hardness softening occurred in Ni irradiated quartzite. Therefore, almost full amorphization occurred in quartz phase that induced large RIVE and large hardness softening. For calcite phase, as reduced GIXRD peaks and radiation softening were observed in marble and limestone, partial amorphization occurred.

This work was funded by the Office of Nuclear Energy, U.S. Department of Energy under Nuclear Energy University Program (NEUP) DE-NE0008882, Project 19-17093.

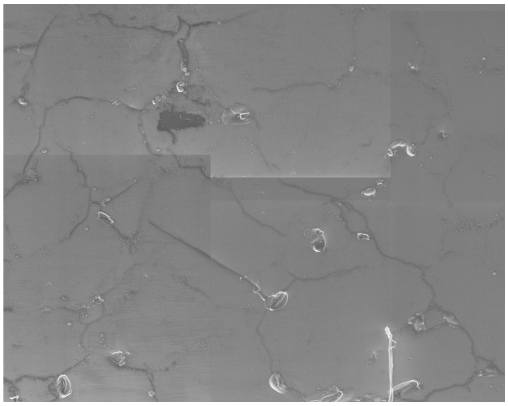

Figure 1. SEM image for Ni irradiated quartzite surface. Irradiation induced cracking and pores formation that mainly along grain boundaries were observed.

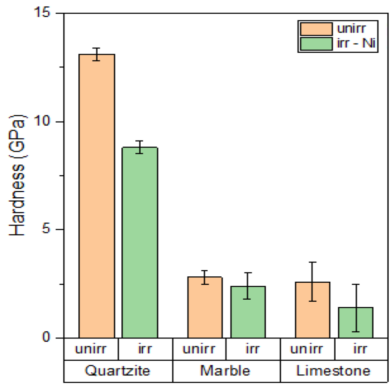

Figure 2. Bulk equivalent hardness values evaluated using Nix-Gao analysis for quartzite, marble and limestone by nanoindentation. Hardness decrease in all samples were observed after Ni irradiation.

EVALUATION OF RADIATION DAMAGE RESISTS OF NUCLEAR WASTE FORM CANDIDATES BY IN-SITU ION IRRADIATION IN THE TF30 TEEM

Kai Sun[1], Fabian Naab[2], and Gary S. Was[1,2]
[1] Department of Materials Science and Engineering, University of Michigan, Ann Arbor, MI48109
[2] Department of Nuclear Engineering and Radiological Sciences, University of Michigan, Ann Arbor, MI48109

Radiation damage in the waste form will occur by gamma decay as well as alpha decay of the TRU elements. The several MeV alpha particle results in a heavy recoil of energy ~0.1 MeV. While much less, the heavy recoil produces many more displacements than does the alpha particle. The nuclear waste forms are in the form of lift-outs of thickness ~100 nm made by focused ion beam (FIB) milling. The 1.2 MeV energy was selected such that the range of the Xe^{3+} ions was greater than the foil thickness. Irradiations were conducted at room temperature with an ion flux of 1.37 $\times 10^{10}$ Xe^{3+}/cm^2s at room temperature. The damage rates for different NWFs are listed in the results. The FIB lift-outs were mounted on a DENSsolutions Wildfire *in situ* heating stage for irradiation in the FEI 300 kV Tecnai G2 F30 TEM operated in diffraction mode. The amorphization doses for the NWF candidates are 0.047 dpa for $Na_3AlCe_6F_{30}$, 0.18 dpa for $Rb_3PrP_2O_8$ and $K_3PrP_2O_8$, 0.21 dpa for $K_3NdP_2O_8$ and 0.22 dpa for $Rb_3NdP_2O_8$, 0.17 dpa for $Na_3NdB_2O_6$, 0.16 dpa for $Na_3Er^{11}B_2O_6$, and 0.26 dpa for $Na_3La^{11}B_2O_6$. Interestingly, the amorphization dose for the heated $Rb_3NdP_2O_8$ is 0.52 dpa.

Support provided by the U.S. Department of Energy, Office of Basic Energy Sciences Award DE-SC0016574 for the Center for Hierarchical Waste Form Materials (CHWM), an Energy Frontier Research Center (EFRC).

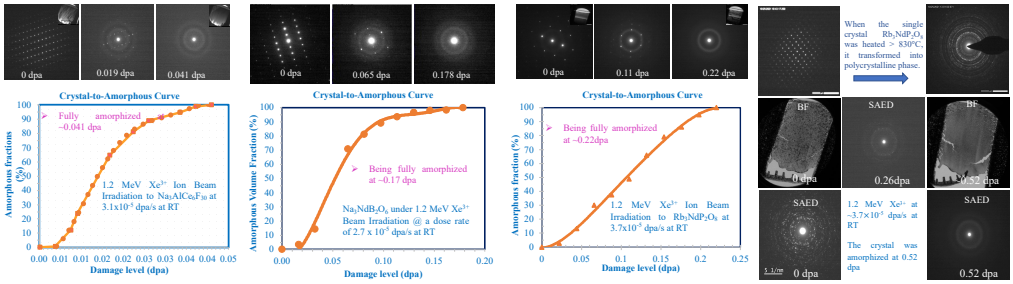

Damage data from the $Na_3AlCe_6F_{30}$, $Na_3NdB_2O_6$, $Rb_3NdP_2O_8$, and the heated $Rb_3NdP_2O_8$, respectively.

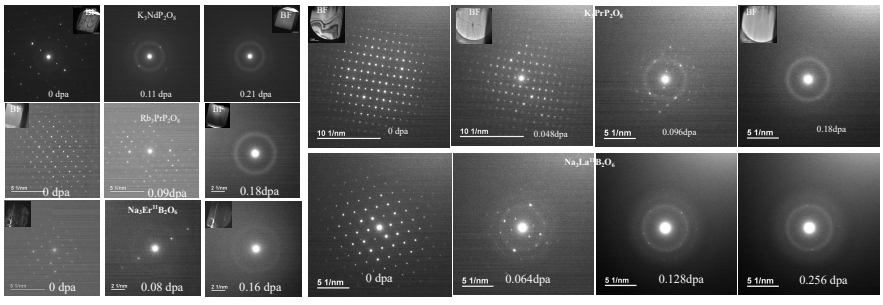

Damage data from the $K_3NdP_2O_8$, $Rb_3PrP_2O_8$, $Na_3Er^{11}B_2O_6$, $Na_3La^{11}B_2O_6$, and $K_3PrP_2O_8$, respectively.

MECHANISMS FOR SOLUTE INCORPORATION IN HIGHLY MISMATCHED $GE_{1-X-Y}SN_XC_Y$

J. Cooper, T. Borrely+, F. Naab*, and R.S. Goldman
Materials Science & Engineering, *Michigan Ion Beam Laboratory
University of Michigan, Ann Arbor MI; +Physics Institute, University of Sao Paulo, Brazil
T. Dey, A. Arbogast, and M. Wistey
Physics, Texas State University, San Marcos TX

Due to the indirect to direct bandgap transitions predicted and observed in $Ge_{1-y}C_y$ and $Ge_{1-x}Sn_x$, $Ge_{1-x-y}Sn_xC_y$ alloys are promising candidates for Si-compatible optoelectronics. For example, dilute GeSn alloys have been utilized for electrically-injected lasers operating at cryogenic temperatures and ultra-dilute GeC alloys with narrowing in the direct bandgap have been reported. Due to the opposing strain effects of Sn and C in Ge, the alloy compositions are difficult to discern using x-ray diffraction measurements, and the mechanisms for Sn and C solute incorporation remain unknown. Here, we report on channeling ion beam analyses of C and Sn incorporation into ~200 nm thick $Ge_{1-x-y}Sn_xC_y$ alloy films grown by molecular-beam epitaxy on Ge substrates. To quantify the Sn composition, we conducted Rutherford backscattering spectrometry (RBS), using a 3 MeV α beam to enable energetically distinct Sn and Ge backscattering yields. Channeling RBS (RBS/c) reveals an increase in the fraction of non-substitutional Sn from 13% to 16% and a decrease in the fraction of displaced Ge atoms from 7% to 5%, as the substrate temperature is increased from 160°C to 200°C. To quantify the C composition in the alloys, we conducted nuclear reaction analysis (NRA) using the $^{12}C(d,p)^{13}C$ reaction. Taking advantage of the energy resonance at 1.2 MeV and the energy stopping power of a 700 nm Ge cap layer, we were able to distinguish the C yields associated with the $Ge_{1-x-y}Sn_xC_y$ films from those of the surface hydrocarbons. In this case, channeling NRA reveals an increase in χ_{min} from 0.2 to 0.5 as the substrate temperature is increased from 160°C to 200°C, suggesting a corresponding increase in non-substitutional C incorporation.

This work is supported by NSF Grant DMR 1810280 and the Michigan Ion Beam Laboratory.

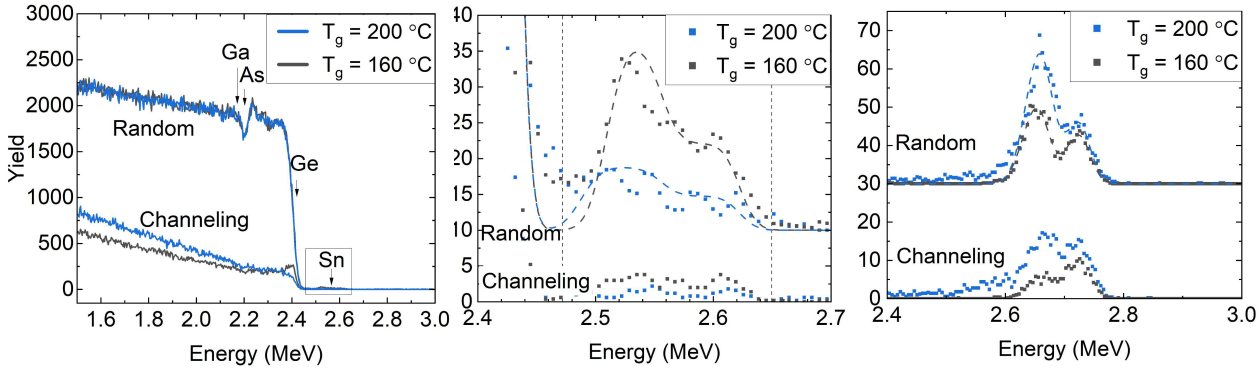

For GeSnC grown at 200°C and 160°C: (a) RBS spectra using 3 MeV α, (b) portion of spectra enclosed in the box in (a) showing the backscattering yield from Sn, (c) NRA spectra using 1.25 MeV D^+ showing the backscattering yield from C.

SIMULATING NEUTRON IRRADIATION DAMAGE IN HT9 WITH HEAVY ION IRRADIATIONS

G. Bruno[1], K. Sun[2], Li He[3], K. G. Field[1]
[1] Department of Nuclear Engineering and Radiological Sciences, University of Michigan
[2] Department of Materials Science and Engineering, University of Michigan
[3] Department of Engineering Physics, University of Wisconsin–Madison, WI, USA

A ferritic-martensitic alloy, HT9, is under consideration as a structural material for advanced reactors. The testing of HT9 within materials test reactors takes several years to meet the appropriate damage levels characteristic of an advanced reactor. Dual ion beams can be used to reach the desired damage levels in a significantly reduced time. By observing the microstructure of the heavy ion irradiated materials, an equivalent set of parameters can be found to emulate the microstructure of neutron irradiated materials from the BOR-60 fast reactor in Russia, which is the goal of these experiments.

Dual ion irradiations were run with 9 MeV Fe^{+++} and 3.42 MeV He^{++} to simulate damage as well as the production of helium within a typical nuclear reactor using a foil degrader to create the desired appm He per dpa profile during irradiation. The irradiation conditions were 16.6 dpa and 33 dpa at 445°C and a 4.3 appm He per dpa ratio. The irradiations conducted this year were both at a dose rate of about 0.0001 dpa/s to look at the formation of Cr-rich α′ precipitation in the microstructure of HT9 at the typical dual ion irradiation conditions.

The samples underwent imaging at the Michigan Center for Materials Characterization at the University of Michigan - Ann Arbor for microstructural features that include cavities and radiation induced segregation. Cavities were imaged with scanning/transmission electron microscopy (S/TEM) techniques [1]. STEM-EDS maps were taken with a Thermo Fisher Talos F200X G2 S/TEM. The figure below shows a representative TEM image of HT9 cavities after a 16.6 dpa irradiation at 445°C, 4.3 appm He per dpa ratio, and at a dose rate of about 0.0007 dpa/s. Initial work toward imaging these microstructural features was completed and quantification is currently in progress.

Primary support for this research was provided by Department of Energy under contract DE-NE0000639.

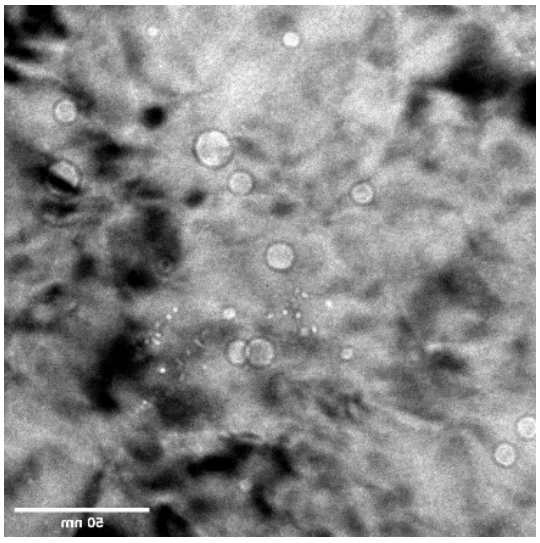

Cavities in HT9 irradiated at 445°C to 16.6 dpa and 4.3 appm He per dpa ratio.

HELIUM IMPLANTATION FOR THE STUDY OF NEUTRINO PRODUCTION TARGET GRAPHITE GRADES UNDER IRRADIATION

Abraham Burleigh[1], Jeff Terry[1,2,3], Kavin Ammigan[4], Frederique Pellemoine[4], Sujit Bidhar[4]
[1] Department of Physics, Illinois Institute of Technology, Chicago IL 60616
[2] Department of Mechanical, Materials, and Aerospace Engineering, Illinois Institute of Technology,
[3] Department of Social Sciences, Illinois Institute of Technology, Chicago IL 60616
[4] Fermi National Accelerator Laboratory, Batavia IL 60510

Polycrystalline, fine-grained graphite is a common material used as neutrino-production accelerator targets where it is exposed to high energy, high intensity proton beams. This results in microstructural damage and eventual bulk material property degradation which can lead to shortened operation lifetimes and premature failures. Future multi-megawatt accelerator facilities and upgrades will continue to increase their primary proton beam power making understanding irradiation effects critical. Helium ion implantation was performed at the Michigan Ion Beam Laboratory (MIBL) as part of a low energy ion irradiation experiment to study relevant graphite grades under irradiation with similar conditions (DPA, temperature and helium content) to neutrino production targets at FNAL.

Two grades of graphite were studied, POCO ZXF-5Q (current FNAL targets) and IG-430 (candidate target material). 8 sets of specimens were implanted with He ions prior to irradiations with 30-36 MeV argon ions at the IRRSUD beamline of the GANIL facility in Caen, France and the ISNAP Facility at the University of Notre Dame to 0.07, 0.27, 0.60 and 0.87 dpa at temperatures of 300 C and 500 C alongside un-implanted specimens. The profile for the highest total helium concentration of 2330 APPM (ave. over 0.35 - 4.6 μm) is shown in Fig. 1. The implantation required 21 different ion energies spanning 70 – 1390 keV with fluences of 3.2 – 5.2x10^{15} ions/cm^2. The projected ranges were calculated using SRIM with a K-P quick calculation, while damage from the argon ions was calculated using MARS and averaged over 0 - 4.6 μm (Bragg peak ~ 10 μm). The implantation was completed in Feb. 2022 with the IRRSUD irradiation (300 C, 0.07 and 0.27 DPA) in Mar. and ND ISNAP (300 C, 0.60 and 0.87 DPA) in Sept. Nanoindentation has been completed on the 0.07 and 0.27 DPA samples and the results are shown in Fig. 2. An increase in elastic modulus and radiation induced hardening were observed in all cases. The elastic modulus shows a plateau from 0.07 – 0.27 DPA while the hardness increases up to 0.27 DPA except for the IG-430 without helium. At low DPA the implanted specimens show increased hardening with similar trends in modulus with and without implantation. TEM examination to observe lattice spacing changes using SAED and defect densities using HREM.

The work was partially supported by the Fermi National Accelerator Laboratory, managed and operated by Fermi Research Alliance, LLC under Contract No. DE-AC02-07CH11359 with the U.S. DOE. This material is based upon work supported by the U.S. Department of Energy, Office of Science, Office of High Energy Physics under an Early Career Award to KA. We acknowledge the GANIL Facility and staff for provision of heavy-ion beams and we would like to thank Clara Grygiel for assistance in using beamline IRRSUD and its instrumentation, and CIMAP for assistance and support in using beamline IRRSUD.

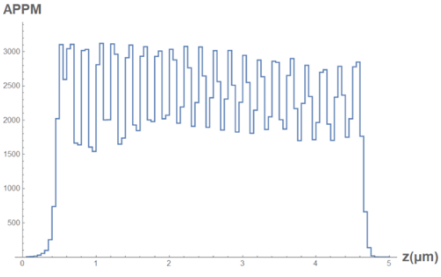

Fig 1. Helium implantation profile achieved at the MIBL in POCO ZXF-5Q and IG-430 graphite.

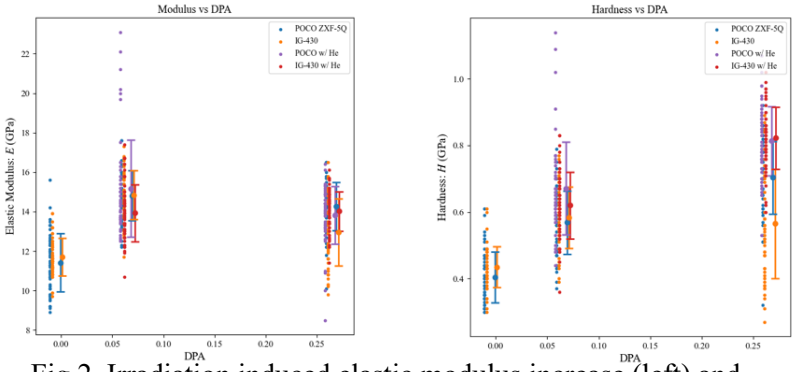

Fig 2. Irradiation induced elastic modulus increase (left) and hardening (right). Data points are offset from the error bars that show 1 standard deviation from the mean.

SELF-ORGANIZATION OF GAS BUBBLE SUPERLATTICE IN METALS AND ALLOYS UNDER ION IMPLANTATION

Cheng Sun[1], Ericmoore Jossou[2], and Jian Gan[1]
[1]Idaho National Laboratory, Idaho Falls, ID 83415.
[2]Brookhaven National Laboratory, Upton, NY 11973.

Self-organization of nanostructures has gained significant interest as a method to fabricate "metamaterials," in which nanocrystals or nanoscale structures serve as building blocks to form an ordered pattern. In the past few decades, many patterned nanostructures have been fabricated. These structures can have novel optical, electronic, magnetic, and photovoltaic properties that may be used for nanodevices, sensors, quantum dots, and radiation-tolerant applications. Understanding self-organization mechanisms is essential to tuning nanopattern formation in a controllable way through a "materials-by-design" approach. The aim of this project is to establish a unified, mechanistic understanding of gas bubble superlattice (GBS) formation under irradiation.

In this work, a series of ion irradiation experiments were performed at the University of Michigan Ion Beam Laboratory (MIBL). Inert gas bubble (He, Ne, Ar, and Kr) superlattices were created in various fcc and bcc metals and alloys (Fe, Ni, W, Mo, W, and W-Re) under ion irradiation. Ion implanter at MIBL was used in this study as it can achieve well-controlled irradiation conditions (ion energy, flux, fluence, and temperature) with inert gas ions. Figure 1 shows an example of He GBS in Fe under irradiation at room temperature. The ion fluence- and temperature-dependent formation of Kr bubble superlattice were investigated in Mo by using both transmission electron microscopy (TEM) and synchrotron-based small-angle X-ray scattering (SAXS). The results show that a critical temperature, fluence, and flux and/or combinations of the implantation parameters are required to promote the formation of solid bubble superlattices (SBS). We also performed Kr implantation in Mo at 300 °C and 400 °C with fluence ranging from 1.5×10^{16} to 1.0×10^{17} Kr/cm^2. Kr SBSs were observed at fluences of 4.5×10^{16} and 1.0×10^{17} Kr/cm^2 at 300 °C as evidenced by the diffraction peaks observed in the 2D SAXS patterns and fast Fourier transform (FFT) from TEM micrographs. At 400°C, the 2D SAXS patterns reveal an early-stage formation of SBSs at fluence of 2.5×10^{16}, 4.5×10^{16}, and 1.0×10^{17} Kr/cm^2. More detailed characterization of irradiated specimens are underway.

This work was sponsored by the U.S. Department of Energy (DOE), Office of Science, Basic Energy Sciences (BES), Materials Sciences and Engineering Division under FWP #C000-14-003. This work was also supported by the U.S. Department of Energy, Office of Nuclear Energy, under DOE Idaho Operations Office Contract DE-AC07-051D14517 as part of a Nuclear Science User Facilities experiment.

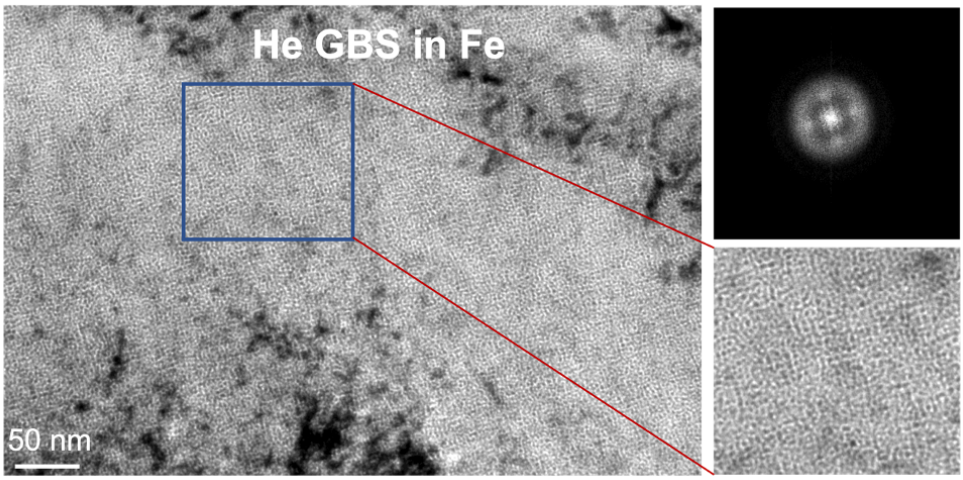

Formation of He GBS in Fe under irradiation at room temperature.

UNDERSTANDING IRRADIATION EFFECTS ON DEFORMATION MECHANISMS IN FE-MN

Y. Zhao[1] and J.P. Wharry[1]
[1] School of Materials Engineering, Purdue University

The objective of this project is to understand how irradiation enables deformation-induced phase transformations in fcc Fe-Mn alloys. In some extreme cases, low-temperature deformation of fcc metals and alloys can occur through martensitic transformations, wherein fcc γ-Fe austenite reverts to hcp ε-martensite or bcc α'-martensite. Irradiation enhances the tendency for martensitic transformations to occur more favorably over conventional dislocation-mediated deformation, which could potentially have severe implications on the performance of load-bearing nuclear reactor structural components. However, the mechanisms underlying the irradiation enhancement of martensitic transformations remain unknown. Specifically, the effects of interstitial-type (e.g. loops) versus vacancy-type (e.g. cavities) irradiation defects on the phase transformation have not yet been deconvoluted.

This irradiation series enables us to determine how the relative populations of vacancy-type and interstitial-type defects modulate deformation-induced martensitic transformations. We prepared and irradiated two sets of specimens of five Fe-xMn alloys, where x = 34, 36, 39, 42, 46 in wt%. We conducted scanning electron microscopy (SEM) based electron backscatter diffraction (EBSD) grain orientation mapping of all specimens before irradiation. The mapped areas were marked with fiducials, and we identified at least one <100>, <101>, and <111> grain that could be identified post-irradiation, as depicted in the figure. The two irradiations conducted were: (1) a bubble-dominated microstructure, using 1 MeV He^+ ions, 500°C, fluence 2 x 10^{16} ions/cm^2; and (2) a defect-dominated microstructure using 2 MeV protons, 300°C, fluence 1 dpa. Next, we will conduct nanoindentation on identified grains, then conduct transmission electron microscopy (TEM) examination of the deformation microstructures.

This work was supported by the U.S. Department of Energy, Office of Science, Basic Energy Sciences, under Award No. DE-SC0020150.

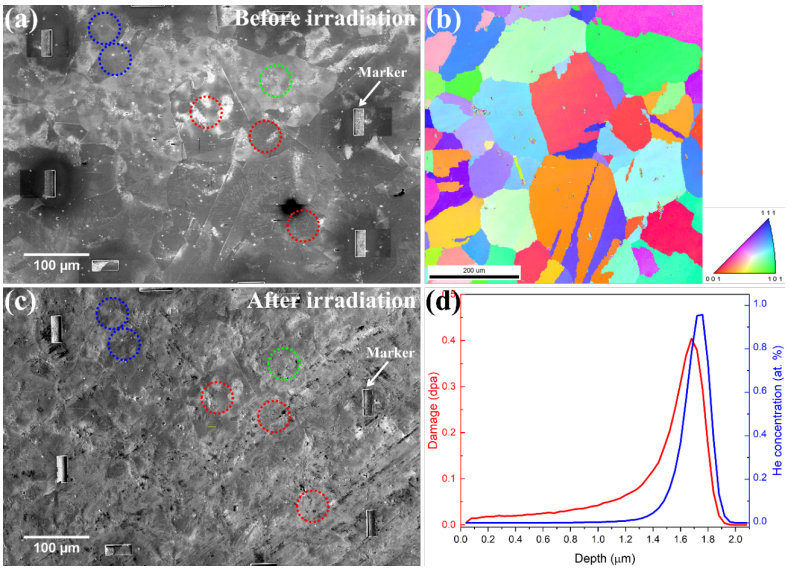

Correlative (a) SEM image and (b) EBSD map identifying grains of interest identified before irradiation on Fe-34Mn specimen; (c) SEM image showing same grains identified after He^+ implantation; (d) SRIM calculation of 1 MeV He^+ implantation.

IRRADIATION EFFECTS ON UNEXPECTED DEFORMATION-INDUCED MARTENSITIC PHASE TRANSFORMATION IN NI ALLOYS

C.D. Clement and J.P. Wharry
School of Materials Engineering, Purdue University

The objective of this project is to understand how irradiation enables deformation-induced phase transformations in fcc Ni-based alloys. Previously unreported martensitic phase transformations have been observed in alloy 625, wherein γ-Ni transforms to ε- HCP martensite and eventually α- BCC martensite consistent with the Bacon-Boger-Olsen-Cohen (BBOC) intersecting shear model. Neutron irradiation has additionally been shown to increase the propensity for this phase transformation to occur by adding obstacles to dislocation motion, which has critical implications to the performance of core reactor structural components. What is currently unknown is the role of specific irradiation defects such as interstitial-type defects (dislocation loops) and vacancy-type defects (cavities). Literature indicates an outsized role for cavities in enhancing the favorability of martensitic phase transformation under mechanical load.

This irradiation series enables us to determine how a loop-dominant irradiated microstructure compares to a cavity-dominant microstructure. We prepared and irradiated two sets of specimens of commercial Ni-alloys (625,690) using two fabrication methods (8 total irradiated specimens). We conducted scanning electron microscopy (SEM) based electron backscatter diffraction (EBSD) grain orientation mapping of all specimens before irradiation. The mapped areas were marked with fiducials, and we identified at least one <101> grain that could be identified post-irradiation, as depicted in the figure. The two irradiations conducted were: 1) a defect-dominated microstructure using 2 MeV protons, 500°C, fluence 1 dpa; and (2) a bubble-dominated microstructure, using 7 energies (200-800keV) He^+ ions, 500°C, fluence 5 x 10^{15} ions/cm^2. Next, we will conduct nanoindentation on identified grains, then conduct transmission electron microscopy (TEM) examination of the deformation microstructures.

This work was supported by the U.S. Department of Energy, Office of Nuclear Energy, Nuclear Science User Facilities, under Award No. 15-8242 and No. 22-4415.

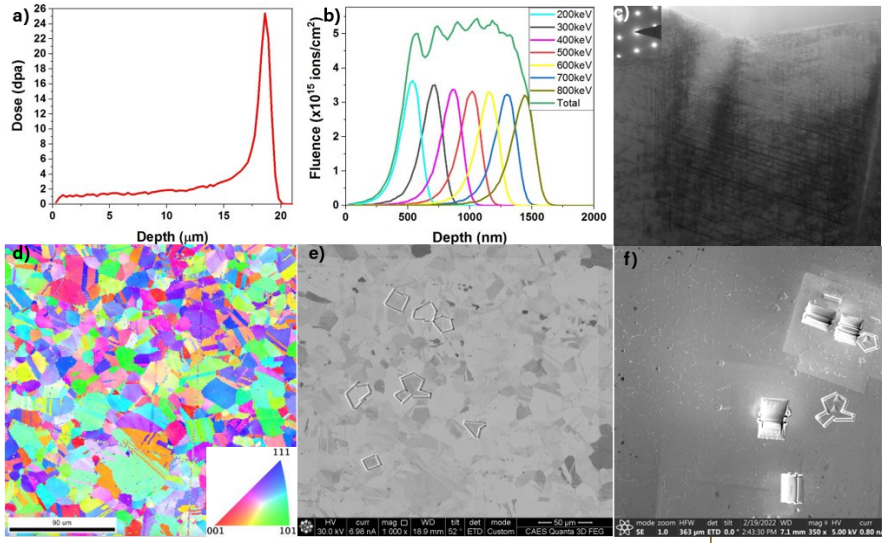

Implantation profiles for a) proton and b) helium irradiations with c) a representative micrograph of alloy 625 He-irradiated and indented <101> grain. d-f) illustrate a correlative IPF of grain structure, and SEM images showing the fiducial marks and indent/liftout of grains of interest.

RESPONSE OF CANDIDATE FUSION BLANKET MATERIALS TO DUAL AND TRIPLE ION IRRADIATION TO UNDERSTAND THE SYNERGIES BETWEEN H, HE AND RADIATION DAMAGE

L. N. Clowers[1], Z. Jiao[1], F. Naab[1], P. Niraula[1], G.S. Was[1]
[1] Department of Nuclear Engineering & Radiological Sciences, University of Michigan

The goal of this study is to investigate the nucleation and growth of cavities and bubbles using multiple ion beams to capture the production of gasses by transmutation in ferritic alloys for fusion blanket materials. To investigate these phenomena, a series of irradiations was conducted on three reduced activation ferritic/martensitic (RAFM) steels; F82H (IEA heat from the National Institutes of Quantum and Radiological Science and Technology in Japan), CNA3 (from ORNL) and Fe8Cr2W (made at Ames laboratory). Ion irradiations were conducted using the 3 MV Pelletron accelerator to provide a defocused beam of 5 MeV Fe^{2+} for irradiation damage, the 1.7 MV Tandetron to provide a raster-scanned beam of 2.85 MeV He^{2+} to be passed through a ~6.4 μm thick Al degrader foil for helium implantation, and the implanter to provide a raster-scanned beam of 390 keV H^{+} through a second ~2.3 μm Al degrader foil for hydrogen implantation. Samples were irradiated in the multi-beam chamber (MBC). A series of dual ion beam (Fe^{2+}+He^{2+}) and triple ion beam (Fe^{2+}+He^{2+}+H^{+}) irradiations were conducted from at 500°C to damage levels of 50, 100, and 150 dpa and damage rates of $2.5x10^{-4}$, ~$1x10^{-3}$, and ~$2.5x10^{-3}$ dpa/s to investigate the dose and dose rate effects of these phenomena. The damage profiles from self-ions and the concentration profiles of injected H/He calculated using a custom Python script along with SRIM-2013 are shown in figure (a). The appm/dpa ratios for helium and hydrogen are 40 appm/dpa and 10 appm/dpa, respectively, at the depth of analysis (500-700nm from the surface). Helium reached 2000 appm and hydrogen reached 500 appm in the region of interest at the end of 50 dpa irradiation at a damage rate of ~$1x10^{-3}$ dpa/s. Thermocouple measurements were used to calibrate the thermal imaging for the temperature determination and were recorded along with pressure and beam current during these irradiation experiments. Post-irradiation microstructural characterization was subsequently performed on focused ion beam (FIB) lift-outs of the irradiated materials via transmission electron microscopy at the Michigan Center for Materials Characterization (MC^2). The cavity microstructure of F82H after triple ion irradiation is shown in figures (b) through (d) where the co-injection of H+ in these irradiations was observed to cause as much as a two-fold increase in the void swelling across each damage level at 500°C through enhanced cavity growth when compared to dual ion irradiation.

This material is based upon work supported by the U.S. Department of Energy, Office of Science, Office of Fusion Energy Sciences under Award Number DE-SC0020226.

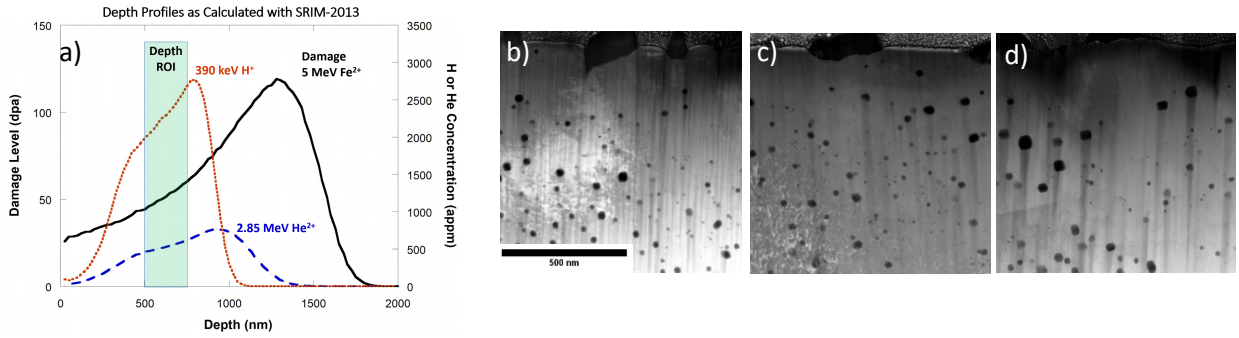

Displacement and implantation curves for 5 MeV Fe^{2+} and energy degraded He^{2+}/H^{+} in F82H RAFM steel (a). STEM-HAADF images of triple ion irradiated F82H at 50 dpa (b) 100 dpa (c) and 150 dpa (d) at 500°C.

PROTON IRRADIATION EFFECT ON CRACK INITIATION BEHAVIOR OF 304L STAINLESS STEEL

J. Ham[1)], S.C. Yoo[2)], and J.H. Kim[3)]
1) Department of Nuclear Engineering, Ulsan National Institute of Science and Technology
2) Korea Institute of Nuclear Safety

Austenitic stainless steel has been widely used in primary circuits of pressurized water reactor. Especially type 304 and 316 stainless steels are the main materials of the reactor internal structures supporting the reactor core. These kinds of structural components are located close to the nuclear fuel of reactor and are irradiated by neutron which causes severe problem irradiation assisted stress corrosion cracking (IASCC). Most of SCC studies have used U-bend specimen in various environment. But U-bend test has a limitation related to its long experimental period. To overcome this weakness, slow strain rate test (SSRT) or constant elongation rate test (CERT) are used which are a kind of acceleration test observing fracture surface. However, in point of view of IASCC, the effect of irradiation is concentrated in the shallow irradiated surface. Thus, it is hard to investigate the effect of irradiation using fracture surface observation method when it comes to deal with crack initiation. In this study, IASCC susceptibility of 304L stainless steel was investigated by conducting SSRT experiments combining with direct current potential drop (DCPD) methodology to detect the exact moment of crack initiation using unirradiated, 1 dpa, and 3 dpa proton irradiated samples respectively.

Proton irradiation had been done from Michigan Ion Beam Laboratory (MIBL) using proton whose beam energy was 2 MeV to a damage level of 1 and 3 dpa at 360 ℃. Each SSRT experiment was conducted until the moment when some remarkable electrical signal was detected from DCPD system. According to the result of experiments whose test environment had been controlled as similar as pressurized water reactor primary circuit, the average crack initiation time of unirradiated samples was about 361 hours, and that of 1 dpa and 3 dpa samples were 253 hours and 213 hours respectively. Proton irradiation did not change the bulk sample's mechanical properties since it affected just shallow depth from the surface, about 20 μm, but the micro-crack initiated on the surface could be detected precisely by DCPD methodology.

This work was financially supported by Korea Hydro & Nuclear Power Co.

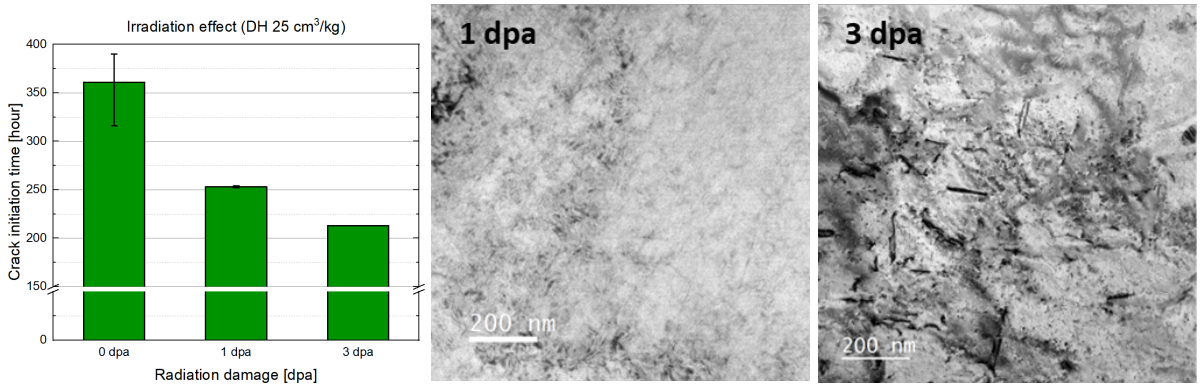

Comparison of crack initiation time measurement depending on the level of radiation damage. The crack initiation happened earlier with unirradiated sample, and the crack initiation time became shorter when the damage level increased from 1 to 3 dpa. According to the transmission electron microscope image of 1 dpa and 3 dpa sample, there is no defects on 1 dpa sample but some defects can be observed from 3 dpa sample.

Cr PATTERNED In625 FOR IN-SITU TEM MOLTEN SALT CORROSION STUDIES

J. Bankson[1], Dr. P. Pragnya[1], Prof. D. Gall[1], Prof. R. Hull[1]
Collaborators: Dr. Emily Liu & group[2] and Dr. Jinsuo Zhang & group[3]
[1]Department of Material Science and Engineering, Rensselaer Polytechnic Institute
[2]Department of Mechanical Engineering, Rensselaer Polytechnic Institute
[3]Department of Nuclear Engineering, Virginia Technical Institute

The next generation of Concentrated Solar Power plants (CSP) will have increased capacities because of molten chloride salts which are cheaper, have lower eutectic melting points, and higher thermal stability range. This project funded by the U.S Department of Energy is to improve the current understanding of corrosion between molten chloride salts ($NaCl - MgCl_2 - KCl$) and the alloy, Inconel 625 (In625). There has been evidence in literature of Cr leading to more severe corrosion of the alloy because of its preferential depletion to form voids, as well as a surface oxide which is broken apart due to the formation of volatile Cr chlorides.

Our objective was to increase local area concentrations of Cr in the In625 through ion implantation so that we can compare corrosion response of standard vs Cr-enriched regions in our in-situ transmission electron microscopy (TEM) experiments. To create patterns of implanted versus non-implanted regions, electron beam lithography was used to create a polymer resist mask above a 75nm film of In625. Figure 1 shows the 0.5 x 0.5um grid pattern. The exposed regions were ion implanted with Cr or Mg at the Michigan Ion Beam Laboratory. SRIM calculations were performed to inform the choice of energy and dose (60 keV, 1.43 x 10^{16} ions/cm^2) so that the max concentration occurs within the In625 film. After the patterned implantation, the TEM sample undergoes a removal process of the polymer mask, electron beam deposition of 3 layers of chloride salts (NaCl, 12 nm $-MgCl_2$, 25.5 nm $-$ KCl, 13.5 nm), and high-temperature molten salt corrosion with a microenvironmental cell TEM holder.

Funding: Department of Energy (DOE) (Grant Number- DoE EERE De-EE0008380).

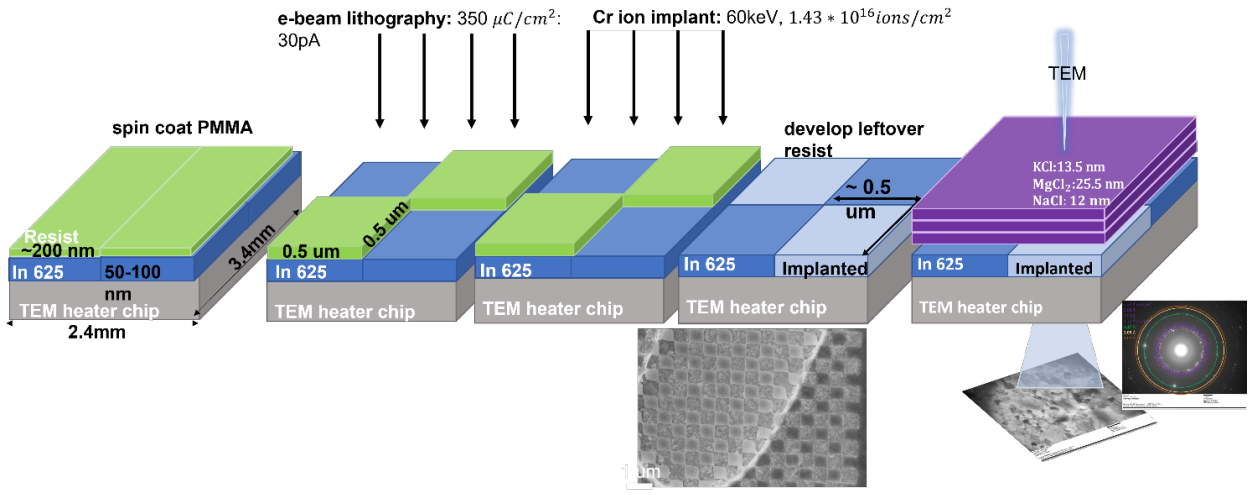

Schematic for the process of electron beam patterning of alloy In625 (SEM micrograph), ion implantation, and the in-situ TEM corrosion experiment where 3 salts are melted to form a ternary eutectic composition.

PHASE DECOMPOSITION IN CRFENIMN MULTI-PRINCIPAL ELEMENT ALLOY

Anshul Kamboj[1] and Emmanuelle Marquis[1]
[1]Department of Materials Science and Engineering, University of Michigan

Multi-principal element alloys (MPEAs) have four or more principal elements in equal or near-equal ratios in solid solutions. CrFeNi-based MPEAs are of particular interest due to their improved irradiation resistance [1], as compared to traditional alloys. However, to be used at high temperatures, these MPEAs must also maintain phase stability. In this study, irradiation is used as an accelerated means to understand phase decomposition in a near-equiatomic $Cr_{18}Fe_{27}Ni_{28}Mn_{27}$ alloys. Three sets of samples were irradiated using 6 MeV Fe^{3+} ions using Wolverine accelerator using a Ni stage heated to 500 ^{0}C. The target damage was 2 dpa and 10 dpa at 700 nm below the surface, achieved using 10^{-4} dpa/s and 10^{-5} dpa/s. Atom probe tomography characterization revealed irradiation accelerated phase decomposition into Cr-rich and Ni-Mn rich precipitates, and Fe-Cr rich matrix (figure). The precipitates coarsened with increase in dose and became ordered with decreasing dose rate.

The work was partly funded by the U.S. Department of Energy Basic Energy Science program, under grant number DE-SC0022980.

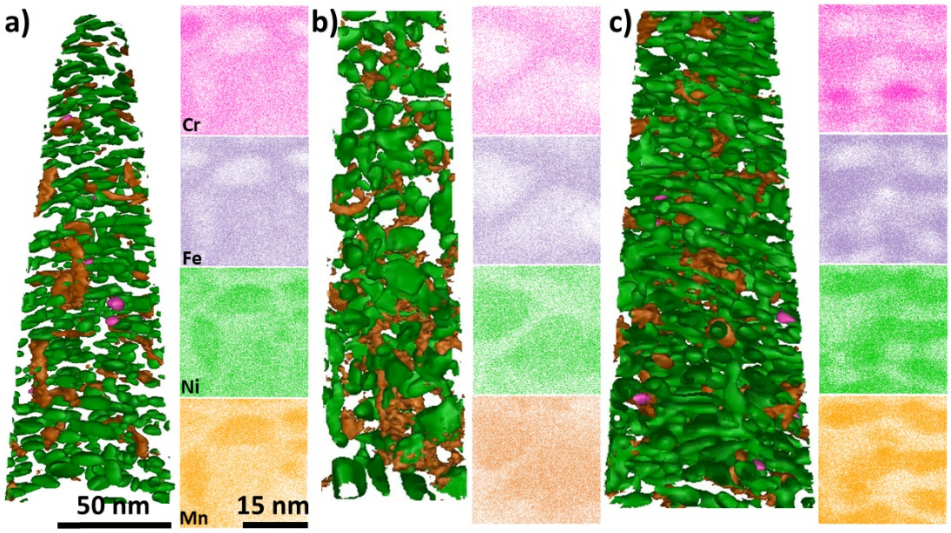

APT reconstruction and element maps from irradiated region showing Ni-Mn rich phase (green), Cr-rich phase (pink), and Fe-Cr rich matrix and dislocation loops (brown) in a) 2 dpa using 10^{-4} dpa/s, b) 10 dpa using 10^{-4} dpa/s, and c) 2 dpa using 10^{-5} dpa/s.

[1] Y. Zhang et. al. Weber, Influence of chemical disorder on energy dissipation and defect evolution in advanced alloys, J. Mater. Res. 31 (2016) 2363–2375.

RADIATION TOLERANCE OF CASTABLE NANOSTRUCTURED ALLOY-9 FOR ADVANCED REACTORS

T.M. Kelsy Green[1], Kevin G. Field[1], Weicheng Zhong[2], Ying Yang[2], Lizhen Tan[2]
[1]Department of Nuclear Engineering & Radiological Sciences, University of Michigan
[2]Oak Ridge National Laboratory

The objective of this project is to observe the dynamic behavior of MX (M=Ti, X=C) nanoprecipitates and helium in a model ferritic/martensitic (F/M) engineering alloy, designated as castable nanostructured alloy-9 (CNA9), through high fidelity ion irradiation experiments. In the year 2022, separate effects testing of the variables of temperature, dose, and dose rate were studied with irradiation experiments found in the table. The behavior of nanoprecipitates is part of an ongoing investigation since 2021. Irradiated samples are being characterized via electron microscopy.

Parameters	Irradiation A	Irradiation B	Irradiation C	Irradiation D	Irradiation E
Ions	9 MeV Fe^{3+}	9 MeV Fe^{3+}	9 MeV Fe^{3+}	9 MeV Fe^{3+}	9 MeV Fe^{3+}
Displacements per atom (dpa)	50	5	15	15	1
Dose rate (dpa/s)	7×10^{-4}	7×10^{-4}	7.15×10^{-4}	7×10^{-4}	7×10^{-4}
Temperature (°C)	300	500	400	600	500
Samples irradiated	ANA2a, ANA2b, CNA-C8, and CNA-C9	ANA2a, ANA2b, CNA-C8, and CNA-C9	CNA-C8 and CNA-C9	CNA8, CNA9, F82H, and Fe8Cr2W	CNA8, CNA9, F82H, and Fe8Cr2W
Source	BL2 Wolverine, Peabody source	BL2 Wolverine, SNICS II	BL2 Wolverine, SNICS II	BL2 Wolverine, SNICS II	BL2 Wolverine, SNICS II

For each irradiation, four samples of F/M steel bars each $10^{L} \times 1.5^{H} \times 1.5\ ^{W}mm^3$ were machined from bulk specimens. Pressure, temperature, and beam currents were recorded during the irradiation experiments. A defocused beam 24 mm^2 in area was used. Figure 1 shows scanning transmission electron microscopy (STEM) bright field (BF) micrographs and STEM-EDS elemental maps of Ti for irradiations C and D.

Samples from these efforts were procured, irradiated, and characterized as part of an FES sponsored Early Career Award (DE-SC0021138).

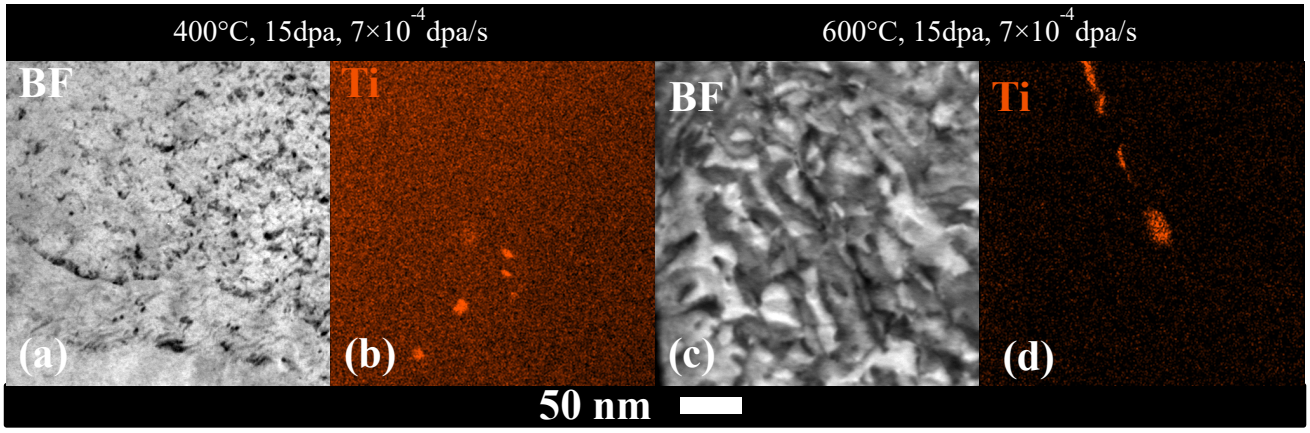

STEM BF (a), STEM-EDS map (b) of Ti of Irradiation C, STEM BF (c), and STEM-EDS map (d) of Ti of Irradiation D.

EXAMINING SPACE WEATHERING OF CARBONACEOUS REGOLITH USING IN SITU ION IRRADIATION AND HEATING EXPERIMENTS IN THE TRANSMISSION ELECTRON MICROSCOPE

D. L. Laczniak[1], M. S. Thompson[1]
[1]Department of Earth, Atmospheric, and Planetary Sciences, Purdue University

Solar wind irradiation and micrometeoroid bombardment are the primary space weathering processes that alter airless planetary regoliths. Analog laboratory experiments are commonly used to constrain the microstructural, chemical, and optical effects of these processes. Ion irradiation experiments that simulate solar wind irradiation and pulsed laser or heating experiments that simulate micrometeoroid impacts are typically performed *ex situ*. However, in the last decade, *in situ* transmission electron microscopy (TEM) has been leveraged to monitor real-time morphological, microstructural, and chemical modifications resulting from simulated space weathering in lunar soils, meteorites, and individual mineral phases. Understanding space weathering of carbonaceous asteroidal regolith is particularly important for maximizing the science return of the Hayabusa2 and OSIRIS-REx missions which have collected samples from the surfaces of C-complex asteroids Ryugu and Bennu, respectively. We performed *in situ* H^+ and He^+ irradiation and subsequent rapid heating on the Murchison CM2 carbonaceous chondrite to investigate the combined effects of progressive solar wind and micrometeoroid bombardment on carbonaceous regoliths.

Murchison dust was crushed into a fine-grained powder, suspended in methanol, and drop-cast onto DENSsolutions Si_3N_4 Wildfire nanochips. Using the *in situ* capabilities of the 200 keV FEI Tecnai G2 F30 TWIN scanning transmission electron microscope (STEM) at the University of Michigan Ion Beam Laboratory (MIBL), we irradiated one sample with 13.2 keV H^+ up to a total fluence of 1.5×10^{17} H^+/cm^2 using a flux of 9.0×10^{12} $H^+/cm^2/s$ and another sample with 23 keV He^+ ions up to a total fluence of 9.0×10^{16} He^+/cm^2 using a flux of 1.4×10^{13} $He^+/cm^2/s$. Following irradiation, each sample was subjected to three consecutive *in situ* rapid heating events. The samples were heated to 1100°C at a rate of ~100°C/s and immediately brought back down to room temperature (21°C). Microstructural changes were evaluated with a combination of bright field (BF) TEM, high-resolution TEM (HRTEM), and selected area electron diffraction (SAED) before and after ion irradiation and the first and third heating events. Chemical analysis was performed by acquiring energy-filtered (EFTEM) and electron energy loss spectroscopy (EELS) maps using the Gatan Continuum ER GIF system. Thus far, results from H^+ irradiation and subsequent rapid heating experiments have been analyzed. Vesiculation was not observed during H^+-irradiation, even after achieving the final fluence of 1.5×10^{17} H^+/cm^2, and partial amorphization of phyllosilicate occurs at a fluence of 8.6×10^{16} H^+/cm^2. Subjecting the H^+-irradiated particles to one rapid heating event causes widespread formation of vesicles (~10-60 nm) and nanoparticles (mostly ≤ ~15 nm). Performing two additional rapid heating events causes existing nanoparticles to coalesce and grow in size.

This work was supported by NASA Solar System Workings Grant 80NSSC19K0960 and the 2021 Microanalysis Society Goldstein Scholar Award. Meteorite samples were allocated by the Buseck Center for Meteorite Studies.

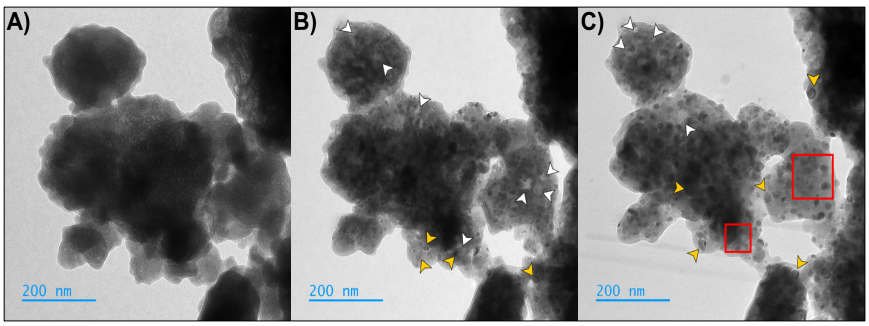

BFTEM images of a Murchison particle after (A) H^+ irradiation, (B) 1x rapid heating, and (C) 3x rapid heating. (A) No vesicles form from H^+ irradiation. (B) White arrows indicate vesicles formed from 1x rapid heating. (C) Red boxes indicate regions where vesicles were destroyed from 3x rapid heating. White arrows denote vesicles. Yellow arrows show examples of subhedral nanoparticles in both (B) and (C).

UNDERSTANDING THE IRRADIATION-INDUCED CORROSION/OXIDATION BEHAVIOR OF EUROFER UNDER CO_2

J. Lim[1], P. Wang[2], G. Was[2]
[1] Materials Business Unit, United Kingdom Atomic Energy Authority, UK
[2] Department of Nuclear Engineering and Radiological Sciences, University of Michigan, USA

With the increase of national interest to focus on developing and deploying clean energy and ensuring a good energy mix for the future, Fusion power plant is one of the ideal candidates. Fusion do not generate carbon dioxide or other greenhouse gases into the atmosphere. Its major by-product is helium gas. Nuclear fusion reactors do not produce high activity, long-lived nuclear waste. The recent record-breaking 59 megajoules of sustained fusion energy demonstrates potential of fusion to be part of the future energy mix at world-leading Joint European Torus facility, a Tokamak-type fusion reactor design, in Oxford, UK [https://www.euro-fusion.org/news/2022/european-researchers-achieve-fusion-energy-record/]. Like any other thermal power plant, coolant/s will be used to transfer heat energy generated from fusion reactions and converted to electrical energy.

This study investigate the corrosion/oxidation behavior of Eurofer under potential coolant candidates for Tokamak-type fusion reactor, i.e. CO_2. Eurofer was irradiated with 5.4MeV proton to a damage level of 0.1dpa at 325°C using a 3 MV National Electronics Corporation Pelletron accelerator in Michigan Ion Beam Laboratory (MIBL). Further post-irradiation analyses will be carried out to examine the impact of irradiation under CO2 at temperature in the UK at Materials Research Facility dedicated for gamma & beta emitting activated materials.

The research used UKAEA's Materials Research Facility, which has been funded by and is part of the UK's National Nuclear User Facility and Henry Royce Institute for Advanced Materials. This work has been funded by the EPSRC Energy Programme [grant number EP/W006839/1]. To obtain further information on the data and models underlying this paper please contact PublicationsManager@ukaea.uk*.

AMORPHIZATION OF LITHIUM OXIDE UNDER HEAVY ION IRRADIATION

D. Muzquiz, S. Raiman
Department of Nuclear Engineering and Radiological Science, University of Michigan.

The DOE-NE has made it a goal to look for improvements in advanced reactor components to increase competitiveness and commercialization of next generation nuclear designs. Similar to other generation four designs, Molten Salt Reactors (MSRs) offer improved thermal efficiency when compared to commercial Light Water Reactors (LWRs). However, graphite moderators used in current reactors are large and inefficient. Earlier experiments done with liquid fueled salts proposed that uncladded graphite had a lifetime of roughly four years, which would require frequent replacement for today's reactors that have lifetimes of 60 to 70 years. Beryllium carbide has shown promising results as a possible material for traditional MSR moderators. However, to implement a new moderating material to the MSR design, the radiation tolerance must be addressed. Preliminary testing with lithium oxide was used as a surrogate for beryllium carbide to see a general overview of how the material responds.

A test was conducted on lithium oxide ceramic to set a top limit for amorphization. Spark Plasma Sintering (SPS) was used to make the sample and minimize its grain size to 81 μm and resulted in a bulk density of 93.6% of its theoretical density. The lithium oxide was baked within the beam line for 3 h at 400 ℃ to remove any moisture that may have between preparation and testing. Following this, the sample was irradiated at 1.5 MeV O^+ ions to a damage level of 50 dpa at 700℃ using the tandem particle accelerator in Michigan Ion Beam Laboratory (MIBL). The total time of exposure was 69.5 h.

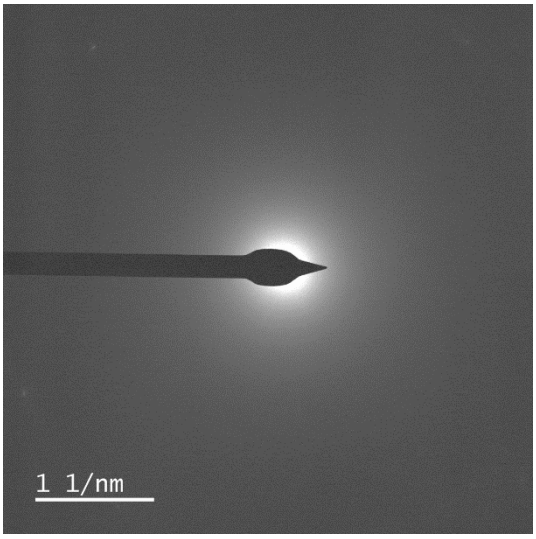

Transmission electron Microscopy (TEM) was conducted by MIBL staff member Kai Sun. The area of analysis was at a depth of 1μm from the surface and was viewed with an electron beam of 200 kV. The result was a magnification of 5700x and showed a hazy light confirming that amorphization did occur.

CORROSION STUDIES ON DUAL BEAM IRRADIATED CR COATED ZR2.5NB MATERIALS AT SMALL MODULAR SUPER CRITICAL WATER OPERATING CONDITIONS

Hygreeva Namburi
Canadian Nuclear Laboratories

Within the CNL's Federal science and technology project, "Establishment of the fuel design for fuel qualification testing of Canadian SCWR fuel" the objective is to determine a promising candidate material for a small-modular supercritical water-cooled reactor (SM-SCWR) fuel cladding. Candidates will be assessed based on their ability to resist corrosion and maintain mechanical integrity, including (among others) acceptable corrosion penetration, oxide thickness, cracking resistance, yield strength, ductility, and resistance to creep. One focus of the project is on Cr-coated zirconium-based claddings, which have high neutron transparency, but uncertain long-term corrosion resistance and mechanical integrity. To study their performance, tests with heavy ion and proton (dual beam) irradiated Cr-coated zirconium-based claddings are planned with the following objectives:

- Determine the effects of irradiation on corrosion behavior
- Determine the effects of irradiation on the microstructure of the Cr coating and the integrity of the interface between the coating and the base alloy, including after short exposures to SM-SCWR conditions
- Determine the effects of irradiation on mechanical integrity of the coating and the interface, including after short exposures to SM-SCWR conditions

The specimens in the present study were irradiated with heavy ions and protons at MIBL to achieve the desired damage depth and dose (dpa) identified. The radiation-induced damage profile and injected ion concentration were estimated by the SRIM-2013 code assuming a displacement threshold energy. The irradiations were performed in compliance with MIBL procedures for ion irradiations and the irradiation conditions are:

- Proton irradiation to 1 dpa, 1 to 1.2 MeV proton beam energy, 450 °C +/- 10 °C, for an area of up to 1.6 cm^2.
- Au irradiations at 15 MeV to achieve 14 dpa, on the same samples.

RADIATION-INDUCED SEGREGATION IN AUSTENITIC FE-BASED CONCENTRATED SOLID SOLUTION ALLOYS

Daniele Fatto Offidani and Emmanuelle Marquis
Department of Materials Science and Engineering, University of Michigan - Ann Arbor

The purpose of this study is to carry out a systematic investigation of radiation-induced segregation (RIS) in austenitic concentrated alloys. The objective is to understand and quantify individual and synergistic chemical interactions as well as the role of microstructure and irradiation conditions on RIS.

In an initial set of experiments, four alloys (Fe-27at.%Ni-10at.%Cr, Fe-27at.%Ni-10at.%Cr-8%Co, Fe-27at.%Ni-10at.%Cr-8%Mn, and equimolar FeNiCrCoMn) were irradiated using 9 MeV Fe^{3+} ions at a $\sim 10^{-4}$ dpa/s dose rate to achieve a damage of 2 dpa at roughly 1200 nm depth from the irradiated surface. The irradiations were performed on a Cu and Ni stage at Forward Looking InfraRed (FLIR) measured temperatures of 300 °C±10°C and 400 °C±10°C respectively using the Wolverine 3 MV Pelletron Accelerator. Following irradiation, the samples were characterized using a combination of scanning electron microscopy (SEM) imaging, electron backscattered diffraction (EBSD) to determine the type of grain boundaries to analyze, and focused ion beam (FIB) milling for producing transmission electron microscopy (TEM) lamellae and atom probe tomography (APT) tips. The TEM lamellae were adopted to acquire sub-nanometer accurate chemical segregation data across the entire damage region at grain boundaries using energy dispersive spectroscopy (STEM-EDS), while the APT tips provided high-fidelity and atomic-scale data for a more modest spatial range.

The chemical analysis of a high-angle grain boundary from the Cantor alloy using STEM-EDS and APT confirmed previously reported results obtained after irradiation under slightly different conditions: a notable enrichment of Ni and Co at the grain boundaries balanced by a substantial depletion in Mn content, as shown in the figure. The analyses of grain boundary chemistry in the FeNiCr, $FeNi_{27}Cr_{10}Co_{8,}$ and $FeNi_{27}Cr_{10}Mn_8$.

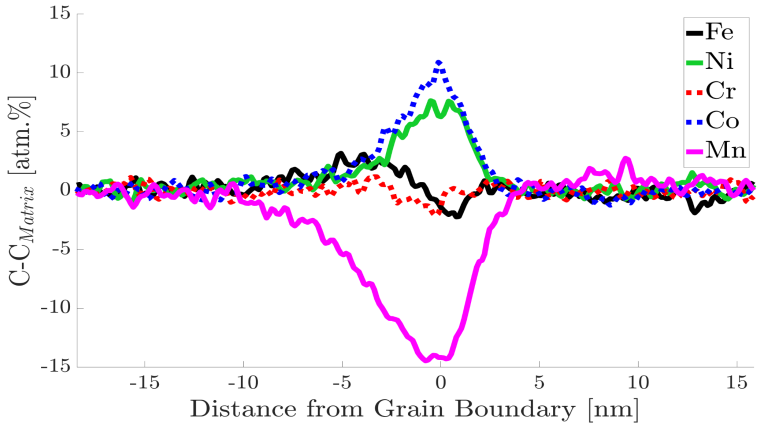

Elemental concentration profiles relative to matrix concentration in irradiated FeNiCrCoMn alloy.

HIGH FIDELITY ION BEAM SIMULATION OF HIGH DOSE NEUTRON IRRADIATION

V. Pauly, Z. Jiao, K. G. Field, G.S. Was
Department of Nuclear Engineering & Radiological Sciences, University of Michigan, Ann Arbor, MI

Traditional research efforts to understand radiation-induced processes in materials require years of comprehensive post-irradiation characterization effort of test-reactor-produced neutron-irradiated material. The same levels of radiation damage can be achieved using heavy-ion irradiation under tightly controlled conditions in days or weeks instead of years in a nuclear reactor, albeit with several challenges because of the time compression. The purpose of this work is to address these challenges in using ion irradiation experiments as a surrogacy for neutron irradiation.

Several dual ion irradiations were performed using 9.0 MeV defocused Fe^{3+} ions to damage the material and simultaneously injecting He^{2+} ions to emulate gas buildup from nuclear transmutation reactions. Bars of 800H steel were dual-ion irradiated to 36 dpa with 0.05 appm He/dpa at 460 and 480 °C and with 0.1 appmHe/dpa at 460 and 500 °C. These specimens were examined with transmission electron microscopy to determine the effects of simultaneous helium injection and radiation damage on the irradiated microstructure of these materials.

This work is supported by the U.S. Department of Energy under award DE-NE0000639. This research was performed, in part, using instrumentation provided by the Department of Energy, Office of Nuclear Energy, Nuclear Technology R&D (formerly Fuel Cycle R&D) Program, and the Nuclear Science User Facilities. The authors acknowledge the University of Michigan College of Engineering for financial support and the Michigan Center for Materials Characterization for use of the instruments and staff assistance.

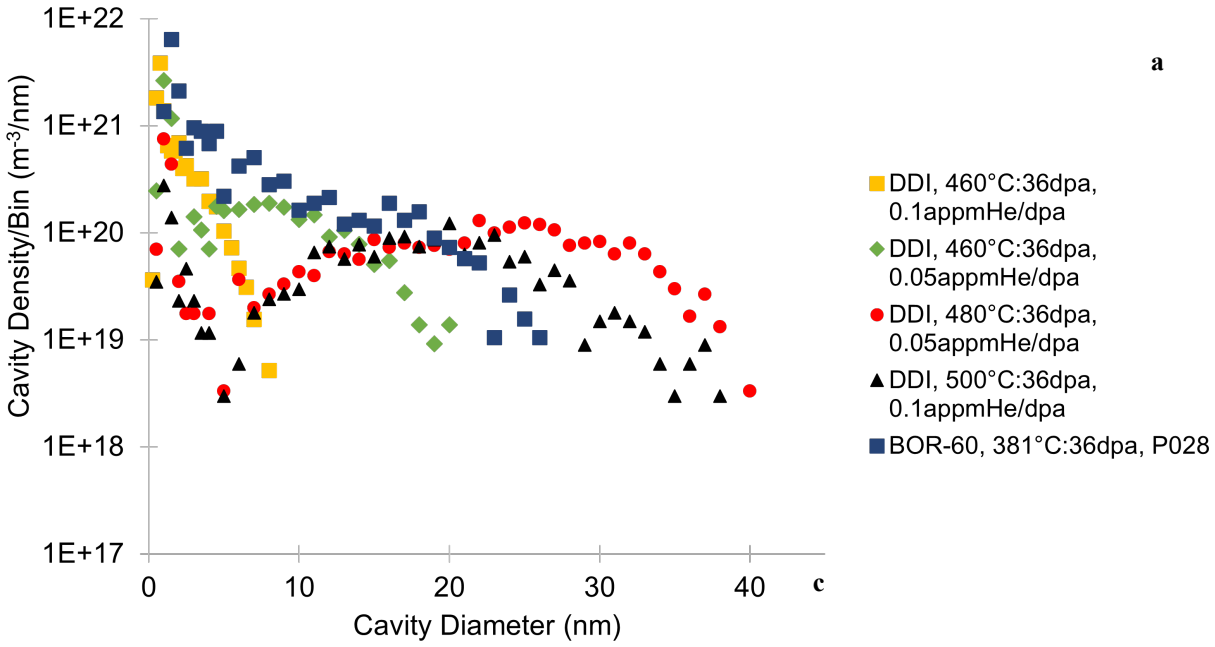

Temperature and He injection level effect on cavity size distributions for dual-ion-irradiated 800H.

IN-SITU PROTON IRRADIATION-CORROSION EXPERIMENT OF BETA-SILICON CARBIDE AT 300°C IN PURE WATER

P. Wang, G. S. Was
Department of Nuclear Engineering and Radiological Sciences, University of Michigan

The objective of this project is to develop a mechanistic understanding of the hydrothermal corrosion behavior of monolithic SiC and SiC/SiC composites in the LWR environment under the influence of water radiolysis products and radiation damage. The project focus on the radiation and radiolysis effects of SiC hydrothermal corrosion on chemical vapor deposited (CVD) β-SiC variants (3C-SiC). The effects of water chemistry and radiolysis products on hydrothermal corrosion will be evaluated via in-situ irradiation-corrosion experiments. The extensive post-test characterization will be performed to determine the dissolution rate of the samples, surface morphology, surface chemical composition, depth profile of SiC from the surface, etc.

In the figure, a series of cross-sectional TEM images of in-situ irradiation-corrosion tested SiC sample, shows the evidence of SiC dissolution under different radiolysis dose rates.

This research was supported by the Department of Energy, Federal Grant #: DE-NE0008781.

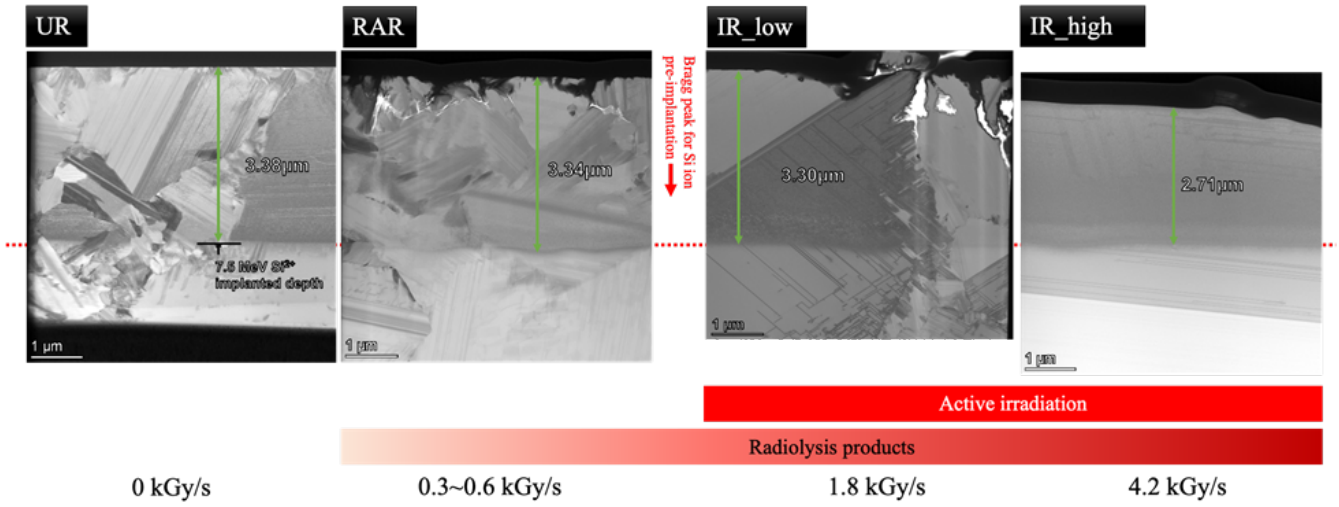

TEM micrographs of the various regions on the in-situ irradiation-corrosion experiment conducted on the 12 dpa pre-irradiated SiC sample, as a function of estimated equivalent dose rate in the water for radiolysis.

IN-SITU PROTON IRRADIATION-CORROSION EXPERIMENT OF PRE-IRRADIATED ZIRCALOY-4

P. Wang[1], B. Kammenzind[2], M. Aumand[3], G.S. Was[1]
[1] Department of Nuclear Engineering & Radiological Sciences, University of Michigan
[2] Navel Nuclear Laboratory
[3]Framatome Inc

The mechanistic understanding of zirconium alloy corrosion in out-of-reactor testing has advanced the state-of-the-art of the field and provided insights into identifying promising alloys for use in reactors under extreme service duty conditions. However, despite similarities between autoclave and in-rector corrosion that allow the use of unirradiated material information and testing to identify potential alloys for service, processes that occur in the reactor are quantitatively and qualitatively different than those in an autoclave environment.

This work assesses the corrosion behavior of proton pre-irradiated Zircaloy-4 sample in simulated LWR reactor environments. Proton pre-irradiations have been performed on Zircaloy-4 samples via isothermal temperature irradiation at 350 °C or two-step proton irradiation to enhance the amorphization of and Fe loss from the laves phase $Zr(Fe,Cr)_2$ precipitates. The as-irradiated microstructures were characterized in an earlier publication [1]. In-situ irradiation-corrosion experiments were then performed on the pre-irradiated samples at 320°C in pure water with various dissolved gases, including hydrogen, nitrogen, and argon, etc. The aim of this systematic investigation of corrosion under influence of active irradiation, existing defect damage, and radiolysis products would offer a better understanding of separate and combined effects on corrosion.

This work was supported by the Navel Nuclear Laboratory and Framatome Inc.

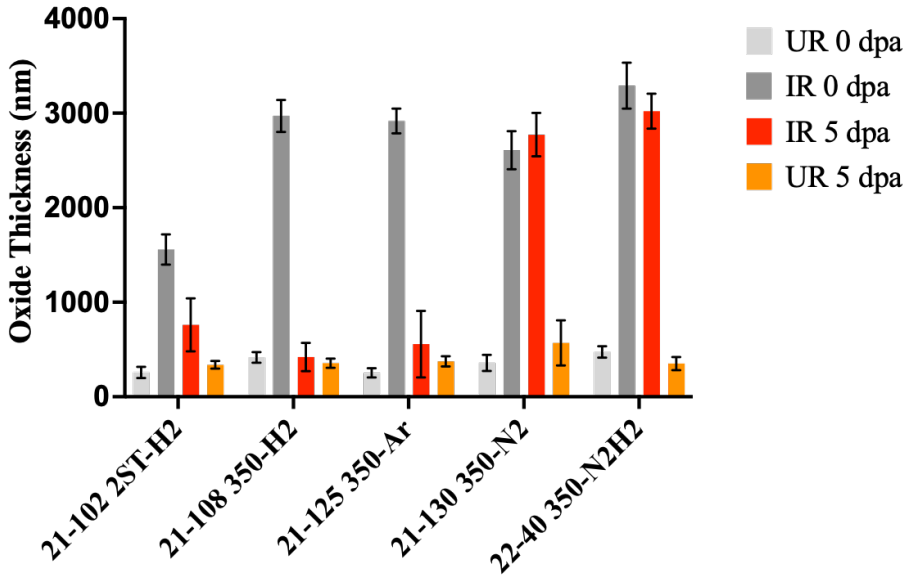

Oxide thickness measurements of in-situ proton irradiation-corrosion experiments, significantly accelerated corrosion has been observed in the irradiated region with active proton irradiation during corrosion in both the pristine and pre-irradiated region of the Zry-4 sample.

[1] P. Wang et al., "Emulation of neutron damage with proton irradiation and its effects on microstructure and microchemistry of Zircaloy-4", J. Nucl. Mat., Vol. 557, 2021, 153281.

ION BEAM ANALYSIS OF SC INCORPORATION INTO ALN

E. Ozdemir[1], J. Cooper[1], F. Naab[2], J. Casamento[3], T. Nguyen[3], D. Jena[3], H. Xing[3], R.S. Goldman[1]
[1]Materials Science & Engineering, [2]Michigan Ion Beam Laboratory
University of Michigan, Ann Arbor MI
[3]Materials Science & Engineering, Cornell University, Ithaca NY

Recently, the incorporation of scandium into wide bandgap semiconductors, such as GaN and AlN, has generated great interest due to the possibility of transforming these pyroelectric materials into promising piezoelectrics and ferroelectrics. GaN and AlN typically crystallize in the wurtzite polytype, with spontaneous polarization along the c-axis. Although the polarization direction can be controlled using Ga- (or Al-) and N-face materials, it is not possible to switch the polarization direction in GaN or AlN without exceeding their dielectric breakdown limit. Alternatively, it has been shown that the incorporation of scandium into AlN and GaN facilitates a piezoelectric response if the wurtzite structure is maintained. ScN typically crystallizes in the rocksalt polytype although metastable WZ polytypes have been reported. To date, the atomistic details of scandium incorporation into GaN and AlN are not well understood. Here, we report on channeling ion beam analyses of Sc incorporation into $Sc_xAl_{1-x}N$ films grown by molecular-beam epitaxy on AlN substrates. Rutherford Backscattering Spectrometry (RBS) measurements were performed using a 1.5 MeV He^{2+} beam to enable energetically distinct Sc and Al backscattering yields. Analysis of the Sc backscattering yields reveals ~70 nm films consisting of 0.05 to 0.30 Sc compositions, consistent with analysis of x-ray diffraction and x-ray reflectivity. Channeling RBS (RBS/c) reveals a nearly monotonic increase in the minimum yields at both the Sc and Al edges, revealing both non-substitutional Sc incorporation and Sc-induced displacement of Al into the [0001] channel. Angular yield scans were collected along the [1120] and [1100] directions for the top 70 nm of the AlN substrate and each of the $Sc_xAl_{1-x}N$ films. For the AlN substrate, high crystallinity is revealed by a low yield in the vicinity of the [0001] channel surrounded by high "shoulders" at angles of ±1.5°. For x_{Sc}=0.05, the minimum [0001] yield increases slightly while the "shoulders" decrease, suggesting atomic displacement into the channel. Significant increases in the minimum [0001] yields are observed for $Sc_xAl_{1-x}N$ layers with x=0.12 and x=0.30 presumably due Sc-induced strain relaxation and to the formation or rocksalt phase AlN inclusions. Monte Carlo-Molecular dynamics simulations of ion channeling are in progress.

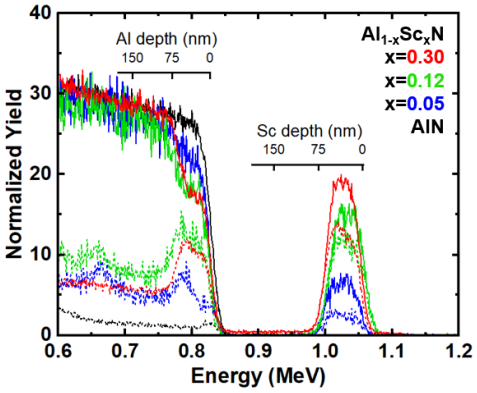

Figure 1. Rutherford backscattering spectra (yield vs. energy) collected from AlN and $Sc_xAl_{1-x}N$ layers with random (solid lines) and channeling (dashed lines) plotted vs. energy. Dashed vertical black lines indicate the top 70 nm used for the angular yield scans in Figure 2.

This work is supported by NSF DMR 1810280, ARPAE #DE-AR0000871, and the Michigan Ion Beam Laboratory.

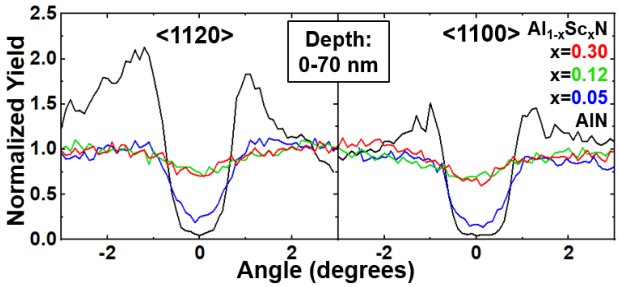

Figure 2. Angular yield scans collected along the <1120> and <1100> directions for the top 70 nm of the AlN substrate and ScAlN layers with x_{Sc} = 0.05, 0.12, and 0.3.

EFFECTS OF THE DOSE AND DEPTH ON THE MICROSTRUCTURAL CHARACTERISTICS OF PROTON-IRRADIATED AUSTENITIC 316 STAINLESS STEEL

Yun Soo Lim, Dong Jin Kim, Min Jae Choi, Seong Sik Hwang, Sung Woo Kim
Materials Safety Technology Development Division, Korea Atomic Energy Research Institute
1045 Daedeok-daero, Yuseong-gu, Daejeon 34057, Korea

Type 316 austenitic stainless steel was irradiated at 360 ℃ with 2 MeV protons to doses up to 6.0 displacements per atom at a depth of approximately 10 ㎛ and the various effects of proton irradiation on the irradiation defects and microstructural changes were characterized using transmission electron microscopy. Irradiation defects produced by protons consisted of Frank loops, network dislocations, voids and nanotwins. The size and the density of the irradiation defects increased depending on the increase of the dose. Frank loops, dislocations and nanotwins were found mainly in regions irradiated to a low dose, whereas voids were dominant in regions irradiated to a high dose. The evolution of representative irradiation defects changed according to the irradiation depth, in agreement with the characteristics of the dose variation depending on the depth. This behavior during the production of distinct irradiation defects according to the irradiation depth appears to be an intrinsic characteristic of any type of ion irradiation. A simple and effective method of preparing TEM specimens to remove chemically the surface damage layers induced by a high-energy focused ion beam and/or low-energy ion milling treatments is suggested.

Funding: This research was financially supported by the Korean Nuclear R&D Programs (RS-2022- 00143718 and 2021M2E4A1037979) through the National Research Foundation of Korea (NRF) funded by the Ministry of Science and ICT.

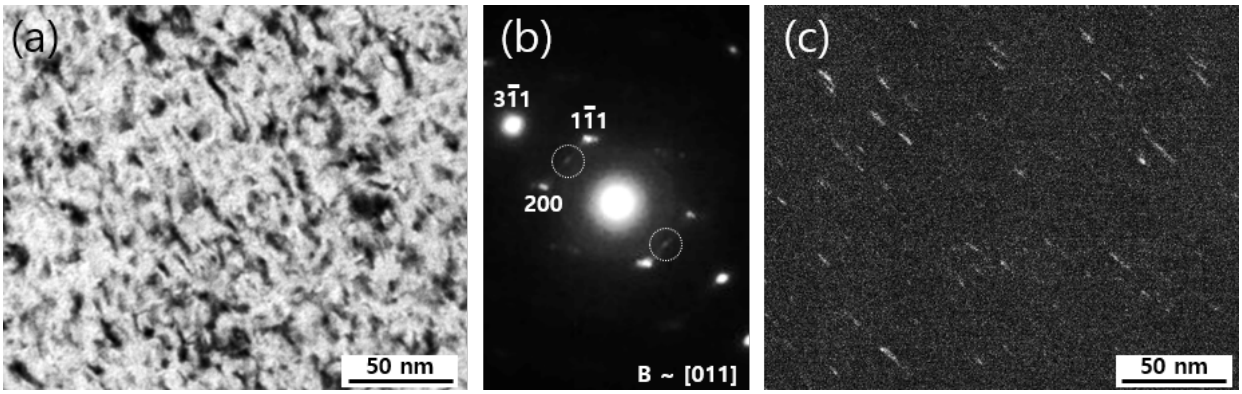

TEM BF (a), SADP (b), and WBDF (c) images of Frank loops taken from the streak enclosed by the white circle in (b) in proton-irradiated 316 SS with a dose of 4.8 dpa.

IN-SITU IRRADIATION CREEP OF 304 STAINLESS STEELS UNDER PROTON IRRADIATION

Arunkumar Seshadri, Marcus E. Parry, Cheng Sun
Idaho National Laboratory, Idaho Falls, ID 83415.

The development of advanced structural materials is key to the implementation of advanced nuclear reactor design concepts, as well as to the life-extension of light-water reactors. Central to the development of new structural material classes is the evaluation of thermal and irradiation creep properties. Traditionally, these properties are measured using bulk specimens held at temperature under static loads for long periods. However, recent advances in thermal and mechanical testing of irradiated materials create an opportunity for the accelerated assessment of small-scale specimens, which can be linked to engineering-scale data. For instance, experimental setup and accelerator technologies unique to the Michigan Ion Beam Laboratory (MIBL) allow for the efficient study of accelerated degradation mechanisms and creep properties of irradiated materials.

Through highly controlled, *in situ* proton irradiation experiments at MIBL, a phased approach was used to establish a mechanistic understanding and isolate the effects of thermal and irradiation creep properties. Two methods were used to measure strain: a laser speckle extensometer (LSE) to optically measure strain with high resolution, and a linear variable differential transducer (LVDT) to monitor total strain from the load cell. 304 stainless steel strips (0.025mm thickness) were be irradiated with 3.5 MeV protons at 450°C to 0.4 dpa. Four experiments were performed under proton irradiation with static applied loads of 200, 250, 285, and 320 MPa, respectively. Beamline Laser alignment was performed before the LSE alignment. The temperature of the sample loading stage was controlled using 3 approaches. Before the irradiation, the stage was heated using the cartridge heater to 450°C. The temperature was controlled by adjusting the applied voltage using a VARIAC. Air flow rate in the cooling channels were also controlled suitably. After the ramp-up to the target temperature of 450 °C, a constant temperature was maintained for 24 hours to obtain a stable temperature. Once the sample was exposed to the proton beam, the applied voltage to the cartridge heater was reduced to account for the temperature increase due to the proton beam. Further temperature control was accomplished at the fine tuning. It took about 1 hour to finetune the sample temperature to achieve the target temperature. Post-irradiation examination of tested 304 stainless steels is being carried out at INL.

This work was sponsored by the Idaho National Laboratory Laboratory-Directed Research and Development Program under Department of Energy (DOE) Idaho Operations Office Contract DE-AC07-051D14517. This work was also supported by the U.S. Department of Energy, Office of Nuclear Energy, under DOE Idaho Operations Office Contract DE-AC07-051D14517 as part of a Nuclear Science User Facilities experiment.

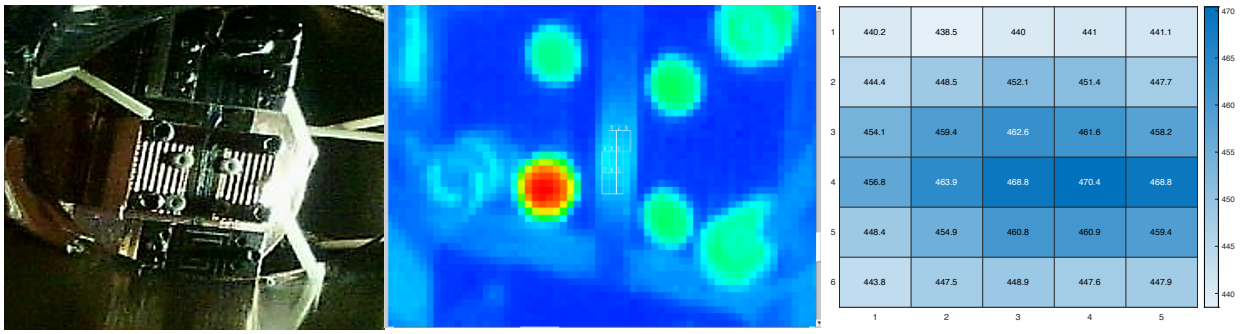

In-situ irradiation creep testing of 304 stainless steels. Protons at energy of 3MeV bombard 304 stainless steel foils at 450°C with applied stresses ranging from 200 to 320 MPa. A uniform 0.4 dpa damage was created in the specimens. The temperature, strain, stress, and beam current were recorded during the irradiation experiments. Primary and secondary creep regions are identified from the creep testing.

DISLOCATION LOOP IN BCC FE AND FECR MODEL ALLOYS DUE TO SELF-ION IRRADIAITON

Yao Li[1], Steven Zinkle[1,2]
[1]Department of Nuclear Engineering, University of Tennessee, Knoxville
[2]Oak ridge national laboratory

Ferritic martensitic (FM) stainless steels are a strong candidate for advanced fission and fusion energy application due to the excellent resistance to irradiation-induced swelling and good resistance to corrosion. However, FM steels face challenges including unacceptably high irradiation-induced hardening and embrittlement at low to intermediate temperatures due to copious formation of dislocation loops and Cr-rich α' precipitates. Although many experiments on FM steels have been performed in past decades, these prior results were not well quantified or interpreted due to resolution limitations of historic scientific instruments.

Two irradiations on Fe, Fe-3Cr, Fe-5Cr, and Fe-8Cr were conducted at 450℃. To minimize the surface effects as well as the implanted ion effects, 8MeV Fe ions were applied in these two irradiations. The ion beam was in defocus beam mode. The irradiations were performed at Michigan Ion Beam Laboratory (MIBL). The total penetration depth is 2350 nm predicted by a computer code called SRIM and the predicted dose level was 0.35 dpa. The dose rates were 10^{-4} dpa/s and 10^{-5} dpa/s. respectively. A self-organization structure called petal-shaped loops was formed due to energetic ions, as shown in the following TEM micrographs. The average diameter of petal-shaped loops in high dose rate irradiation was much smaller than the one in low dose rate irradiation (118 nm vs 260 nm). More details will be available in a journal article.

Research sponsored by the Office of Fusion Energy Sciences, U.S. Department of Energy under contract DE-AC05-00OR22725 with UT-Battelle, LLC and grant # DE-SC0023293 with the University of Tennessee. The ultra-high purity Fe and Fe-Cr samples were supplied by the EUROfusion consortium.

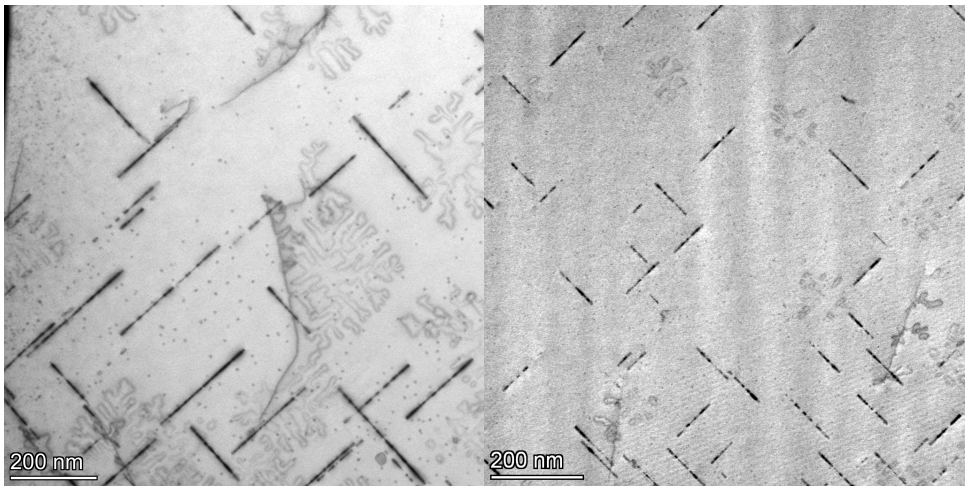

Fe-8Cr irradiated to 0.35 dpa at 450 ℃ and 10^{-5} dpa/s (left), and Fe-8Cr irradiated to 0.35 dpa at 450 ℃ and 10^{-4} dpa/s (right). The STEM micrographs were taken under on-zone condition, B = 001.

TEACHING

NERS 425 LABORTORY ON NUCLEAR REACTION ANALYSIS

M. Atzmon, F. Naab and Z. Jiao
Department of Nuclear Engineering and Radiological Sciences, University of Michigan

For one of the modules in the NERS 425 course, students conducted an experiment to determine the stoichiometry of a TixNy sample using the reaction between a deuterium particle and a nitrogen nucleus: N14(d,α)C12. Nuclear reaction analysis (NRA) is a well-established surface analysis technique. In this method, an energetic particle (deuterium – produced by the Tandem accelerator at MIBL) interacts with the nucleus of an N atom in the target to give a reaction product (α particle) that can be measured. The students also use the backscattered yield from an RBS experiment to determine the amount of Ti in the sample by implementing simulation codes like RUMP or SIMNRA with the given experimental spectrum.

In the first meeting, prior to the experiment, a short tutorial was given to the students on the accelerator, electronics, detectors, software, and vacuum components. After that, they worked independently with just the basic support from the MIBL staff (required in the setup of the ion beam and the collection of the spectra). The students decided on a few parameters of the experiment (beam energy, time for spectrum acquisition, etc.), and obtained spectra similar to the ones in the figure.

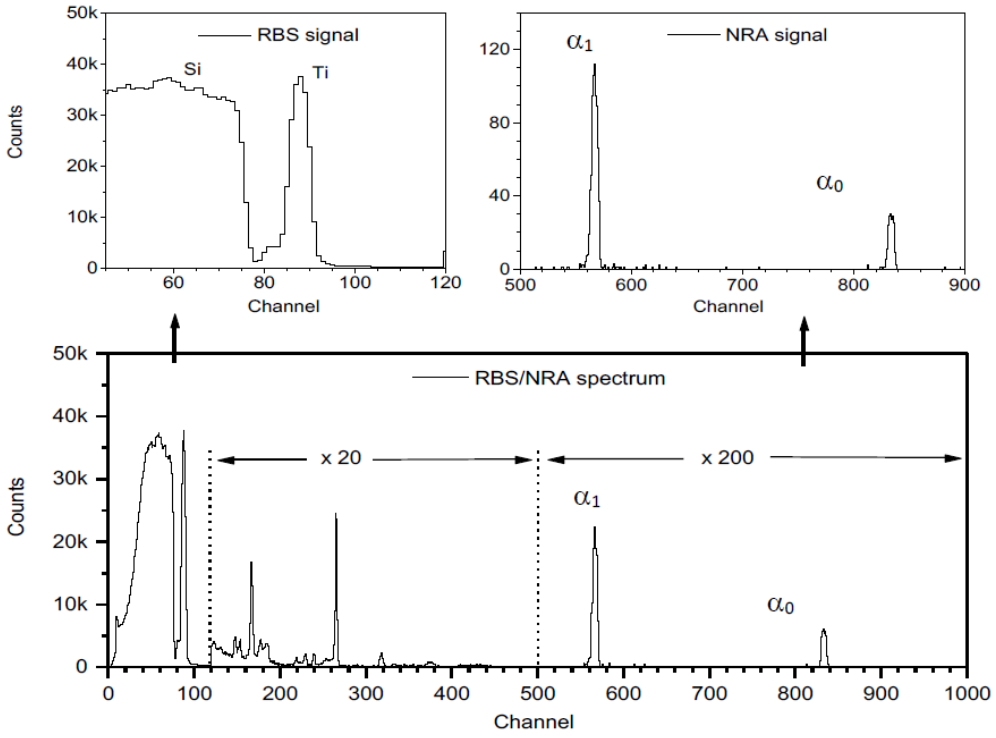

Typical RBS/NRA spectrum for the TiN film obtained during class. Conditions: beam energy: 1.4 MeV D^+, solid angle 5 msr., detector angle 150°.

PUBLICATIONS AND PRESENTATIONS

Publications

1. J. Bowman, P. Wang, G. S. Was, M. Bachav, A. T. Motta, "Ion irradiation induced amorphization of precipitates in Zircaloy," J. Nucl. Mater. 571 (2022) 153988. https://doi.org/10.1016/j.jnucmat.2022.153988.

2. A. T. Hines, G. Morrison, H. B. Tisdale, M. D. Smith, T. M. Besmann, A. Mofrad, M. Aziziha, R. E. Booth, K. Sun, G. S. Was, H-C zur Loye, "Crystallization of $A_3Ln(BO)_3)_2$ (A-Na, K; Ln – Lanthanide) from a Boric Acid Containing Hydroxide Melt: Synthesis and Investigation of Lanthanide Borates as Potential Nuclear Waste Forms," Inorg. Chem. 61 (2022) 11232-11242. https://doi.org/10.1021/acs.inorgchem.2c01301.

3. Y. J. Cho, K. Sun, G. Was, K. Lu, "In-situ microstructure observation of oxidized SiC layer in surrogate TRISO fuel particles under krypton ion irradiation," J. Alloys Comp. 920 (2022) 165833.

4. H. B. Tisdale, M. S. Christian, G. Morrison, T. M. Besmann, K. Sun, G. S. Was, H.-C. zur Loye, "Investigation of Rare Earth-Containing Double Phosphates of the Type $A_3Ln(PO_4)_2$ (Ln – Y, La, Pr, Nd, and Sm-Lu) as Potential Nuclear Waste Forms, Chem. Mater. 34 (2022) 3819-3830.

5. L. Clowers, Z. Jiao, G. S. Was, "Synergies between H, He and radiation damage in dual and triple ion irradiation of candidate fusion blanket materials," J. Nucl. Mater. 565 (2022) 133722.

6. S. Levine, C. Pareige, Z. Jiao, P.D. Edmondson, G. S. Was, S. J. Zinkle, A. Bhattacharya, "Phase instabilities in austenitic steels during particle bombardment at high and low dose rates," Mater. & Design 217 (2022) 110588.

7. S. Levine, C. Pareige, Z. Jiao, P.D. Edmondson, G. S. Was, S. J. Zinkle, A. Bhattacharya, "Data on Cu- and Ni-Si-Mn-rich solute clustering in a neutron irradiated austenitic stainless steel," Data in Brief, 42 (2022) 108263.

8. S. Taller, V. Pauly, Z. Jiao, R. Hanbury, G. S. Was, "Solute segregation and precipitation across damage rates in dual-ion-irradiated T91 steel," J. Nucl. Mater. 563 (2022) 153626.

9. W. Kuang. X. Feng, D. Du, M. Song, M. Wang, G. S. Was, "A High-resolution Characterization of Irradiation-assisted Stress Corrosion Cracking of Proton-irradiated 316L Stainless Steel in Simulated Pressurized Water Reactor Primary Water," Corr. Sci. 199 (2022) 110187.

10. P. Wang, K. Nowotka, G. S. Was, "Reproducing Shadow Corrosion on Zircaloy-2 using In-situ Proton Irradiation," J. Nucl. Mater. 558 (2022) 153406.

11. J. Ham, S.C. Yoo and J.H. Kim, "Effect of Dissolved Hydrogen Concentration on Irradiation Assisted Stress Corrosion Cracking Initiation Properties of Stainless Steel in Primary Water Condition", Transaction of Korean Nuclear Society Autumn Meeting, Changwon, Korea, October 2022.

12. Kamboj A., Marquis E., "Effect of dose rate on the phase stability of CrFeNiMn MPEA", Scripta Materialia (2022), 215, 114697. https://doi.org/10.1016/j.scriptamat.2022.114697.

13. Jiang, B., Liang, N., Xu, L., Gao, L., Peng, Q., Jiao, Z., Qiao, L. "Combined effects of irradiation and hydrogen on the mechanical and corrosion performances of the ferrite in duplex phase steels". Journal of Nuclear Materials, 572(2022)154069

14. Jiang, B., Liang, N., Peng, Q., Lin, X., Jiao, Z., Xu, L.,Qiao, L. "Irradiation-induced corrosion tendencies evolution at the phase boundaries containing carbides in duplex stainless steel." Corrosion Science, 208(2022)110662

15. P. Xiu, C.P. Massey, T.M.K. Green, S. Taller, D. Isheim, N. Sridharan, K.G.Field, Microchemical evolution of irradiated additive-manufactured HT9, Journal of Nuclear Materials, Volume 559, 2022, ISSN 0022-3115, https://doi.org/10.1016/j.jnucmat.2021.153410.

Conference Proceedings / Presentations

1. "On the Path to Understanding Stress Corrosion Crack Initiation of Austenitic Alloys in High Temperature Water," Symposium on Seeing is Believing – Understanding Environmental Degradation and Mechanical Response using Advanced Characterization Techniques, TMS Annual Meeting, Anaheim CA, March 2022.

2. "Synergistic Processes in Irradiation-Corrosion of Materials in High Temperature Water," Symposium on Synergistic Irradiation, Corrosion, and Microstructural Evolution in Nuclear Materials, TMS Annual Meeting, Anaheim CA, March 2022.

3. "Synergies between H and He in Irradiation-induced Swelling in Candidate Fusion Blanket Materials," Symposium on Materials Systems for the Future of Fusion Energy, TMS Annual Meeting, Anaheim CA, March 2022.

4. "Degradation of Materials in Extreme and Complex Environments," Symposium on Mechanical Behavior and Degradation of Advanced Nuclear Fuel and Structural Materials, TMS Annual Meeting, Anaheim CA, March 2022.

5. "Effect of Cascade Size and Damage Rate on a' Precipitate Stability in Fe-15Cr," NuMAT, The Nuclear Materials Meeting, Elsevier, Ghent, 2022.

6. "Extension of Radiation Damage in Flux Thimble Tubes using Heavy Ions," NuMAT, The Nuclear Materials Meeting, Elsevier, Ghent, 2022. ***INVITED***

7. "Mechanistic Understanding of Irradiation Assisted Stress Corrosion Cracking," 20th International Conference on Environmental Degradation of Materials in Nuclear Power Systems – Water Reactors, AMPP, Snowmass, July 2022. ***INVITED***

8. "Crack Initiation Testing of Neutron-irradiated Type 347 Stainless Steel in Simulated PWR Water with LiOH or KOH," 20th International Conference on Environmental Degradation of Materials in Nuclear Power Systems – Water Reactors, AMPP, Snowmass, July 2022.

9. "Effect of Potassium Hydroxide Primary Water Chemistry on the IASCC Behavior of 304 Stainless Steel," 20th International Conference on Environmental Degradation of Materials in Nuclear Power Systems – Water Reactors, AMPP, Snowmass, July 2022.

10. "Effect of Proton Irradiation on Microstructure and Microchemistry of Zircaloy-4," 20th International Conference on Environmental Degradation of Materials in Nuclear Power Systems – Water Reactors, AMPP, Snowmass, July 2022.

11. "Acceleration of 316L Stainless Steel Corrosion by Proton-irradiation-induced displacement damage in hydrogenated steam," 20th International Conference on Environmental Degradation of Materials in Nuclear Power Systems – Water Reactors, AMPP, Snowmass, July 2022.

12. "Synergistic Processes in Irradiation-Corrosion of Materials in High Temperature Water," Symposium on Synergistic Irradiation, Corrosion, and Microstructural Evolution in Nuclear Materials, TMS Annual Meeting, Anaheim CA, March 2022. ***INVITED***

13. J. Ham, S.C. Yoo and J.H. Kim, "[Invited talk] Effect of Water Chemistry Changes on Irradiation Assisted Stress Corrosion Cracking Behavior of Stainless Steels in Primary Water Environment", Symposium on Water Chemistry and Corrosion in Nuclear Power Plants in Asia, 2022, Online, Japan, September 2022.

14. Kamboj A., Marquis E., "Microstructure of a CrFeNiMn alloy under ion irradiation", 2nd world congress on High Entropy Alloy, Charlotte, 2022.

15. P Wang, GS Was, "$Zr(Fe,Cr)_2$ Precipitate Amorphization and Iron Redistribution in Zircaloy-4 using a Two-step Proton Irradiation," The 20th International Conference on Environmental Degradation of Materials in Nuclear Power Systems-Water Reactor, AMPP Publishing, ED22-17211-SG, (2022).

16. F Pellemoine, C Wheldon, GS Was, S Meigo, I Monnet, C Grygiel, M Calviani, B Zwaska, A Gottberg, C Barbier, Y Sun, Y Chiu, E Getto, A Alessi, CS Cutler, D Woodley, F Boix Pamies, P Wang, A Couet, S Bidhar, M Freer, O Toader, F Naab, Y Dai, D Winder, D Kim, K Ammigan, M Moorhead, D McClintock, S Taller, T Ishida, S Raiman, N Moncoffre, K Kriewaldt, "arXiv: Irradiation Facilities and Irradiation Methods for High Power Target," FERMILAB-CONF-22-124-AD, 2022/3/15 (2022).

17. F Pellemoine, C Barbier, Y Sun, K Ammigan, S Bidhar, B Zwaska, D McClintock, S Taller, D Winder, CS Cutler, D Kim, Y Chiu, M Freer, C Wheldon, A Gottberg, F Boix Pamies, M Calviani, N Moncoffre, S Meigo, T Ishida, Y Dai, A Couet, K Kriewaldt, M Moorhead, GS Was, O Toader, F Naab, P Wang, D Woodley, E Getto, S Raiman, C Grygiel, I Monnet, A Alessi, "Irradiation Facilities and Irradiation Methods for High Power Target," arXiv preprint arXiv:2203.08239, (2022).

18. K. Nowotka, Hoffmann P., A. Hasselbach, R. Geier, S. Gray, P. Wang, G. S. Was, "ULTRAFLOW Shield: A New Spacer Grid Coating for BWR Fuel," TopFuel 2022 Light Water Reactor Fuel Performance Conference, Raleigh, NC, 2022/10

19. Peng Wang, Gary S Was, Izabela Szlufarska, Luke Czerniak, Keyou Mao, "Mechanistic Understanding of Radiolytically Assisted Hydrothermal Corrosion of SiC in LWR coolant Environments," OSTI ID: 1907417, 2022/12/29 (2022).

20. P. Wang, G. S. Was, "$Zr(Fe,Cr)_2$ Precipitate Amorphization and Iron Redistribution in Zircaloy-4 using a Two-step Proton Irradiation," The 20th International Conference on Environmental Degradation of Materials in Nuclear Power Systems-Water Reactor, Snowmass CO, June 17-21, (2022).

21. Q. Chen "Microstructural evolution and hardness changes in ion irradiated Ni-based superalloys", Symposium on Novel Materials and Properties, TMS Annual Meeting, San Diego, March 2022.

22. K.G. Field, P. Patki, N. Sharaf, L. Hawkins, M. Lynch, R. Jacobs, D. Morgan, L. He, C.R. Field. Real-time, On-Microscope Automated Quantification of Features in Microcopy Experiments Using Machine Learning and Edge Computing. *Microscopy and Microanalysis, 28*(S1), 2046-2048. (2022) doi:10.1017/S1431927622007929

23. P. Xiu, H. Bei, Y. Zhang, L. Wang, K.G. Field, Towards Optimized Characterization of Dislocation Loops in Irradiated FCC Alloys Using On-Zone STEM Techniques. Microscopy and Microanalysis,

Volume 28 (S1), 2022, 2070-2071. doi:10.1017/S1431927622008017

24. K.G. Field, P. Patki, K. Sun, W.Y. Chen, T.M.K. Green, R. Renfrow, M. Shen, R. Jacobs, D.D. Morgan, N. Saraf, C.R. Field, Development and Demonstration of a Real-Time Machine Vision Platform for *In-Situ* Microscopy, Presentation at the Materials Research Society Conference, Honolulu, HI, USA, May 2022

25. K.G. Field, T.M.K. Green, R. Renfrow, W. Zhong, T. Graening, P. Patki, W.Y. Chen, N. Sridharan, L. Tan, Y. Yang, Towards a Fundamental Understanding of Transmutation Effects in US-Developed Nanostructured Fusion Relevant Steels, Presentation at the Technology of Fusion Energy (TOFE) Conference, Anaheim, CA, USA, June 2022

26. K.G. Field, P. Xiu, S. Taller, N. Sridharan, "Tailored Radiation Responses of an Additively Manufactured Ferritic/Martensitic Steel", Invited presentation at NuMat, Ghent, Belgium, October 2022. ***INVITED***

27. K.G. Field, P. Patki, M. Lynch, R. Jacobs, T.M.K. Green, R. Renfrow, W.Y. Chen, D.D. Morgan, C.R. Field, "Recent Innovations in Machine Learning-based Techniques for In-Situ Microscopy Data Analysis", Invited presentation at MS&T, Pittsburgh PA, USA, October 2022. ***INVITED***

28. K.G. Field, F. Gao, T.R. Allen, E. Marquis, Z. Jiao, G. Was, B. Wirth, S. Zinkle, A. Motta, Accessing the High Damage Regime with Ion Irradiation in the SNAP Program, presentation at the GAIN workshop as part of the ANS summer meeting, Anaheim, CA, USA, June 2022. ***INVITED***

29. K.G. Field, P. Patki, K. Sun, W. Y. Chen, T.M.K. Green, R. Renfrow, M. Lynch, M. Shen, R. Jacobs, D.D. Morgan, C.R. Field, Real-time, On-Microscope Automated Quantification of Features in Microscopy Experiments Using Machine Learning and Edge Computing, Presentation at International Workshop on Transmission Electron Microscopy with in-situ Irradiation, Ann Arbor, MI, USA, July 2022.